CATALYTIC CONVERSION OF METHANE AND CARBON DIOXIDE IN CONVENTIONAL FIXED BED AND DIELECTRIC BARRIER DISCHARGE PLASMA REACTORS

ISTADI

UNIVERSITI TEKNOLOGI MALAYSIA

CATALYTIC CONVERSION OF METHANE AND CARBON DIOXIDE IN CONVENTIONAL FIXED BED AND DIELECTRIC BARRIER DISCHARGE PLASMA REACTORS

ISTADI

A thesis submitted in fulfilment of the
requirements for the award of the degree of
Doctor of Philosophy

Faculty of Chemical and Natural Resources Engineering
Universiti Teknologi Malaysia

JUNE 2006

Specially dedicated to my beloved mother and father,
my beloved wife Warti Istadi, my daughter Aisyah Muthmainah Istadi,
and my beloved son Ridwan Firdaus Istadi

ACKNOWLEDGEMENT

Alhamdulillah, Praise to Allah, first and foremost, I would like to express my sincere and deep appreciation to my supervisor, Prof. Dr. Nor Aishah Saidina Amin, for her advise, mentoring, guidance and support on the project.

I would like to thank all CREG members for their support and friendship over these years. In particular, Chong Chee Ming, Soon Ee Peng, Tutuk, Tung Chun Yaw, Sriraj Ammasi, Kusmiyati, Siti Kartina, Tirena Siregar, Zaki and Didi Dwi Anggoro are greatly acknowledged for their helpful discussions and suggestions. I wish them all much future success. Special thanks go to Ms. Shamsina Sabdin (PRSS), Dr. Putut Marwoto, and Dr. Agus Setia Budi for their help in performing the catalyst characterizations.

Financial support received in the forms of a research grant (Project number: 02-02-06-0016 EA-099, Vot 74005) from the Minstry of Science, Technology and Innovation (MOSTI), Malaysia is gratefully acknowledged, as it allowed me to focus all my efforts on research.

I would like to thank all laboratory technicians in particular Mr. Latfie and Mr. Bidin for their assistance and cooperation throughout the research work, also to all the administration personnel in the Faculty of Chemical and Natural Resources Engineering, Universiti Teknologi Malaysia.

Finally, to my wife, Warti Istadi, and my daughter, Aishah M. Istadi and my son, Ridwan F. Istadi, for the endless encouragement throughout these years.

Lastly, thanks to everyone that I have previously mentioned and to everyone who I may have unintentionally not recognized.

ABSTRACT

The natural gases in the Natuna and Arun fields have CO_2/CH_4 ratio being 71/28 and 15/75, respectively. These ratios are potential for the production of C_{2+} hydrocarbons and synthesis gas. The purpose of this study is to develop a new catalytic process for CH_4 and CO_2 utilization to produce C_2 hydrocarbons and/or synthesis gas at high conversion and selectivity. The studies started with a thermodynamic equilibrium analysis of CH_4 and CO_2 reactions to produce C_2 hydrocarbons and synthesis gas in order to investigate the feasibility of the reactions thermodynamically. The results showed that carbon dioxide reforming of methane, reverse water gas shift reaction, and dehydrogenation of ethane to ethylene were more viable than CO_2 oxidative coupling of methane. In the catalytic system, CeO_2-based catalyst screening was performed. The CaO-MnO/CeO_2 catalyst system displayed high stability suitable for the CO_2 oxidative coupling of methane. Moreover, the operating parameters, such as the CO_2/CH_4 feed ratio and reactor temperature, and the catalyst compositions, such as wt% CaO and wt% MnO, were optimized by using Weighted Sum of Squared Objective Functions algorithm. The synergistic effect of basicity and reducibility towards the catalytic activity were also addressed using XRD, CO_2-TPD and H_2-TPR. The synergistic effect of catalyst basicity and reducibility are vital in enhancing the reaction performance. Since the conversion and yield were still low, the conventional CO_2 oxidative coupling of methane was replaced with a more advanced reactor. The hybrid catalytic dielectric-barrier discharge plasma reactor was utilized for the synthesis gas and C_{2+} hydrocarbons (ethane, ethylene, acetylene, and propane) production in one step. The new reactor system displayed promising performance at low temperature over CaO-MnO/CeO_2 catalyst. Next, a hybrid Artificial Neural Network – Genetic Algorithm technique was used to facilitate modelling and optimization of the plasma reactor system for both non catalytic and catalytic dielectric barrier discharge plasma reactors. It was found that the catalytic dielectric barrier discharge plasma reactor performed better performance than the non-catalytic one and the conventional fixed bed reactor. The main products from the plasma reactor were ethane, carbon monoxide, propane, and hydrogen, while the minor products were ethylene and acetylene.

ABSTRAK

Gas semulajadi di kawasan Natuna dan Arun mempunyai nisbah karbon dioksida kepada metana iaitu 71/28 dan 15/75. Nisbah ini amat berpotensi bagi penghasilan hidrokarbon C_2, gas sintesis dan juga bahan kimia lain yang bernilai tinggi. Tujuan penyelidikan ini adalah untuk membangunkan satu proses bermangkin yang menggunakan gas metana dan karbon dioksida sebagai bahan mentah untuk menghasilkan hidrokarbon C_2 dan/atau gas sintesis dalam penukaran bahan mentah serta kepemilihan hasil yang tinggi. Penyelidikan ini bermula dengan analisis imbangan termodinamik ke atas tindak balas metana dan karbon dioksida terhadap penghasilan hidrokarbon C_2 dan gas sintesis untuk menentukan sama ada tindak balas ini adalah munasabah dari sudut termodinamik atau tidak. Keputusan menunjukkan bahawa tindak balas pembentukan semula metana menggunakan karbon dioksida, tindak balas anjakan berbalik air-gas, penyahhidrogenan etana kepada etena adalah lebih berpotensi berbanding dengan tindak balas penggandingan oksigen dengan metana menggunakan karbon dioksida. Oleh itu, pelbagai mangkin berasaskan serium oksida ditapis untuk memilih mangkin yang paling sesuai bagi tindak balas itu. Mangkin CaO-MnO/CeO_2 didapati paling sesuai untuk tindak balas tersebut disebabkan kestabilannya. Tambahan pula, parameter tindak balas seperti nisbah suapan iaitu nisbah karbon dioksida kepada metana dan suhu reaktor serta komposisi mangkin seperti peratus berat kalsium oksida dan peratus berat mangan oksida yang paling optimum turut disiasat dengan menggunakan algoritma Weighted Sum of Squared Objective Functions. Kesan sinergistik kebesan dan kebolehturunan terhadap prestasi mangkin juga dinyatakan dengan menggunakan XRD, CO_2-TPD dan H_2-TPR. Didapati kesan sinergistik kebesan dan kebolehturunan mangkin memainkan peranan yang penting dalam meningkatkan prestasi tindak balas penggandingan oksigen dengan metana menggunakan karbon dioksida. Disebabkan penukaran bahan mentah dan penghasilan adalah rendah, proses penggandingan oksigen dengan metana menggunakan karbon dioksida yang konvensional digantikan oleh suatu reaktor yang lebih canggih. Reaktor plasma yang menggunakan nyahcas dielektrik-rintangan hibrid bermangkin dicadangkan untuk penghasilan gas sintesis dan C_{2+} hydrokarbon (etane, etena, etuna dan propana). Sistem reaktor baru ini menunjukkan prestasi yang lebih menjanjikan pada suhu rendah di atas mangkin CaO-MnO/CeO_2. Dalam sistem reaktor ini juga, suatu teknik rangkaian saraf buatan dan algoritma genetik hibrid digunakan untuk memudahkan proses pemodelan dan pengoptimuman sistem kedua-dua reaktor plasma yang menggunakan nyahcas dielektrik-rintangan hibrid bermangkin dan tidak bermangkin. Didapati bahawa reaktor plasma bermangkin menunjukkan prestasi yang lebih baik berbanding dengan reaktor plasma tanpa mangkin dan menunjukkan prestasi yang lebih baik pula berbanding dengan reaktor berdasar tetap konvensional. Hasil utama dari reaktor plasma bermangkin ini ialah etana, karbon monoksida, propana dan hidrogen manakala hasil sampingan adalah etena dan etuna.

TABLE OF CONTENTS

CHAPTER	TITLE	PAGE
	TITLE	i
	DECLARATION	ii
	DEDICATION	iii
	ACKNOWLEDGMENT	iv
	ABSTRACT	v
	ABSTRAK	vi
	TABLE OF CONTENTS	vii
	LIST OF TABLES	xiv
	LIST OF FIGURES	xvii
	LIST OF ABBREVIATIONS	xxvi
	LIST OF SYMBOLS	xxviii
	LIST OF APPENDICES	xxxi
1	**INTRODUCTION**	1
	1.1 Methane and Carbon Dioxide Utilization	1
	1.1.1 Carbon Dioxide Reforming of Methane	5
	1.1.2 Carbon Dioxide Oxidative Coupling of Methane	6
	1.2 Current Catalyst Technology in CO_2 OCM	7
	1.3 Basic Principles of Heterogeneous Catalysis	11
	1.3.1 Concept of Catalysis	11
	1.3.2 Point Defects in the Catalyst Structure	14
	1.3.3 Role of Acid-Base Properties in Catalytic Oxidation	15

1.3.4 Surface Oxygen Species and Their Role in Selective Oxidation 16
1.3.5 Cerium oxide as a Catalyst for CO_2 OCM 17
1.4 Problem of Research 19
1.5 Objectives of Research 20
1.6 Scopes of Research 21
1.7 Organization of Thesis 21

2 RESEARCH METHODOLOGY 23
2.1 Materials of Research 23
2.2 Research Methodology 24
2.2.1 General Research Methodology 24
2.2.2 Catalysts Preparation 28
2.2.3 Catalysts Characterization 30
2.2.3.1 Structure of Catalyst Bulk using X-Ray Diffraction (XRD) 30
2.2.3.2 Structure of Catalyst Surface using Fourier Transform Infra Red 31
2.2.3.3 Structure of Catalyst Surface using Raman Spectroscopy 32
2.2.3.4 Catalyst Basicity by CO_2 Temperature-Programmed Desorption (CO_2-TPD) 33
2.2.3.5 Catalyst Surface Reducibility by H_2-Temperature-Programmed Reduction (H_2-TPR) 34
2.2.4 Catalysts Testing in Conventional Fixed Bed Reactor 34
2.2.4.1 Experimental Rig 34
2.2.4.2 Testing Procedure and GC Program 37
2.2.4.3 Analysis of Products Composition 38
2.2.4.4 Calculation of Conversion, Selectivity and Yield 39

2.2.5 Experimental Rig of DBD Plasma Reactor 41

3 THERMODYNAMIC ANALYSIS OF CO-GENERATION OF C_2 HYDROCARBONS AND SYNTHESIS GAS FROM METHANE AND CARBON DIOXIDE 46

3.1 Introduction 46

3.2 Technique for Calculation of Thermodynamic Chemical Equilibrium 48

3.2.1 Equations Used in Chemical Equilibrium Computation 49

3.2.2 Chemkin Technique for Equilibrium Computation 52

3.2.3 Equilibrium Performances Calculation Method 52

3.3 Standard Gibbs Free Energy Change Analysis of CH_4 and CO_2 Reactions 53

3.4 Effect of Temperature on Equilibrium Mole Fraction, Conversion, Selectivity and Yield without Carbon 57

3.5 Effect of CO_2/CH_4 Feed Ratio on Equilibrium Mole Fraction, Conversion, Selectivity and Yield Without Carbon 62

3.6 Effect of System Pressure on Equilibrium Mole Fraction, Conversion, Selectivity and Yield Without Carbon 65

3.7 Effect of Temperature and CO_2/CH_4 Feed Ratio on Carbon and No Carbon Formation Regions at Equilibrium 68

3.8 Summary 69

4	**SCREENING AND STABILITY TEST OF CATALYST FOR CARBON DIOXIDE OXIDATIVE COUPLING OF METHANE TO C_2 HYDROCARBONS**	71
	4.1 Introduction	71
	4.2 CeO_2-Based Catalysts Screening for CO_2 OCM Reaction	71
	4.3 Surface Structure of CeO_2-Based Catalysts	74
	4.4 Stability Test of Catalyst for CO_2 OCM Reaction	80
	4.5 Summary	80
5	**SYNERGISTIC EFFECT OF CATALYST BASICITY AND REDUCIBILITY ON THE PERFORMANCE OF TERNARY CeO_2-BASED CATALYST FOR CO_2 OCM PROCESS**	82
	5.1 Introduction	82
	5.2 X-Ray Diffraction (XRD) Characterization	83
	5.3 Surface Basicity/Base Strength Distributions of Catalysts by CO_2-TPD	85
	5.4 Surface Reducibility of Catalysts by H_2-TPR	87
	5.5 Catalyst Activity for CO_2 OCM and its Correlation with Catalyst Basicity and Reducibility	90
	5.4 Summary	93
6	**OPTIMIZATION OF PROCESS PARAMETERS AND CATALYST COMPOSITIONS IN CARBON DIOXIDE OXIDATIVE COUPLING OF METHANE OVER CaO-MnO/CeO_2 CATALYST**	94
	6.1 Introduction	94
	6.2 Design of Experiment and Statistical Analysis Method	97
	6.2.1 Central Composite Design	97
	6.2.2 Model Fitting and Statistical Analysis Method	100
	6.2.3 Canonical Analysis of Stationary Point	101

6.3 Theory for Multi-Responses Optimization Technique 102
6.4 Additional Criterion for Determination of Final Optimal Responses 106
6.5 Algorithm of WSSOF Technique in Multi-Responses Optimization 107
6.6 Single-Response Optimization of Catalytic CO_2 OCM Process 110
6.6.1 Single-Response Optimization of Methane Conversion 110
6.6.2 Single-Response Optimization of C_2 Hydrocarbons Selectivity 116
6.6.3 Single-Response Optimization of C_2 Hydrocarbons Yield 121
6.7 Multi-Responses Optimization of Catalytic CO_2 OCM Process 126
6.7.1 A Hybrid Numerical Approach of WSSOF Technique 126
6.7.2 Effect of Weighting Factor Variations on Pareto-Optimal Solution 127
6.7.3 Generation of Pareto-Optimal Solution in Multi-Responses Optimization 130
6.7.4 Location of Optimal Process Parameters and Catalyst Compositions in Multi-Responses Optimization of CO_2 OCM 133
6.7.5 Simultaneous Optimization of C_2 Selectivity and Yield in CO_2 OCM 135
6.7.6 Simultaneous Optimization of CH_4 Conversion and C_2 Selectivity in CO_2 OCM 137
6.7.7 Simultaneous Optimization of CH_4 Conversion and C_2 Yield in CO_2 OCM 138
6.8 Experimental Verification and Benefit of Multi-Responses Optimization in CO_2 OCM Process 139
6.9 Summary 141

7	**A HYBRID CATALYTIC – DIELECTRIC BARRIER DISCHARGE PLASMA REACTOR FOR METHANE AND CARBON DIOXIDE CONVERSIONS**	142
	7.1 Introduction	142
	7.2 Principles of Dielectric-Barrier Discharge Plasma Reactor	144
	7.2.1 Gas Breakdown in Dielectric-Barrier Discharge Plasma Reactor	146
	7.2.2 Influence of Dielectric Material Properties in DBD Plasma Reactor	147
	7.2.3 Interaction of Gas Discharge and Catalyst in DBD Plasma Reactor	149
	7.3 Recent Modelling on Catalytic Dielectric-Barrier Discharge Plasma Reactor	150
	7.4 A Hybrid Artificial Neural Network - Genetic Algorithm (ANN-GA) for Modelling and Optimization	151
	7.4.1 Artificial Neural Network (ANN)-Based Modelling	152
	7.4.2 Genetic Algorithm (GA)-Based Optimization	158
	7.5 Experimental Design for Training Data	166
	7.6 Typical Waveform of High Voltage Power Supply and Plasma Discharge	169
	7.7 Possible Reaction Mechanism of CH_4 and CO_2 Conversion in Hybrid Catalytic – DBD Plasma Reactor	170
	7.8 Modelling and Optimization of DBD Plasma Reactor without Catalyst Using Hybrid ANN-GA Strategy	171
	7.8.1 Artificial Neural Network Model Development for MIMO System	171
	7.8.2 ANN Simulation for the Effect of Operating Parameters in DBD Plasma Reactor Without Catalyst	177

7.8.3 Multi-Responses Optimization of DBD Reactor Plasma Without Catalyst using Hybrid ANN-GA Strategy 182
7.9 Modelling and Optimization of Catalytic DBD Plasma Reactor Using Hybrid ANN-GA Strategy 190
7.9.1 Artificial Neural Network Model Development for MIMO System 190
7.9.2 Effect of Hybrid Catalytic-Plasma DBD Reactor for CH_4 and CO_2 Conversion 193
7.9.3 ANN Simulation for the Effect of Operating Parameters in Catalytic DBD Plasma Reactor 195
7.9.4 Multi-Responses Optimization of Catalytic DBD Plasma Reactor using Hybrid ANN-GA Strategy 202
7.10 Comparison between DBD Plasma and Conventional Fixed Bed Reactors at the Same Feed Flow Rate and Catalyst 209
7.11 Summary 211

8 CONCLUSIONS AND RECOMMENDATIONS 212
8.1 Conclusions 212
8.2 Recommendations 214

REFERENCES 216
APPENDICES 232

LIST OF TABLES

TABLE NO.	TITLE	PAGE
1.1	Gas reserves in Malaysia	2
1.2	Composition of natural gas (in % vol.) from various locations	2
1.3	Catalyst development for methane oxidative coupling with carbon dioxide to C_2 hydrocarbons	9
2.1	Materials were used for catalysts preparation	23
2.2	Gas materials were used for reactant and carrier	24
3.1	The possible reactions of CH_4 and CO_2 considered in the thermodynamic analysis	49
3.2	Standard Gibbs free energy change (ΔG_T^o) of the reactions at various temperature	55
3.3	Equilibrium constant (K value) of the reactions at various temperature	56
3.4	Effect of CO_2/CH_4 feed ratio on equilibrium performances	64
4.1	Catalysts performance results of CeO_2-based catalyst and comparison with previous researchers (pressure = 1 atm, catalyst weight = 2 gram, and total feed flow rate = 100 cm^3/min)	73
4.2	Vibration mode of Raman and FT-IR spectra of various CeO_2-based catalysts	77
5.1	Distribution of basic sites number determined by CO_2-TPD expressed in μmol CO_2 desorbed / g cat based on the different basicity strengths	86

TABLE NO.	TITLE	PAGE
5.2	Catalysts performance results of CeO_2-based catalysts (T = 1127 K, CO_2/CH_4 = 2, weight of catalyst loaded = 1 g, total feed flow rate = 50 cm^3 min^{-1})	92
6.1	Experimental ranges and levels of factors or independent variables	98
6.2	Experimental design matrix in their natural values and experimental results	99
6.3	ANOVA results for CH_4 conversion model	112
6.4	Multiple regression results and sorted significance effect of regression coefficient for CH_4 conversion model	113
6.5	ANOVA results for C_2 hydrocarbons selectivity model	117
6.6	Multiple regression results and sorted significance effect of regression coefficient for C_2 hydrocarbons selectivity model	118
6.7	ANOVA results for C_2 hydrocarbons yield model	122
6.8	Multiple regression results and sorted significance effect of regression coefficient for C_2 hydrocarbons yield model	123
6.9	Simultaneous optimal multi-responses of C_2 selectivity and yield and the corresponding factors location	136
6.10	Simultaneous optimal multi-responses of CH_4 conversion and C_2 selectivity and its corresponding factors location	138
6.11	Simultaneous optimal multi-responses of CH_4 conversion and C_2 yield and its corresponding factors location	139
6.12	Experimental verification of the final optimal point in multi-responses optimization of C_2 selectivity and yield	140
7.1	Characteristic of non-thermal discharges	145
7.2	Central Composite Design with full factorial design for the DBD plasma reactor without catalyst	166
7.3	Central Composite Design with fractional factorial design for the catalytic DBD plasma reactor	166
7.4	Experimental design matrix of DBD plasma reactor without catalyst	167

TABLE NO.	TITLE	PAGE
7.5	Experimental design matrix of catalytic DBD plasma reactor	168
7.6	Experimental data of DBD plasma reactor without catalyst at low temperature	173
7.7	Additional data of DBD plasma reactor without catalyst at potential operating conditions and comparison with that at pure CH_4 as feed	174
7.8	Comparison of various ANN structures for 1 hidden layer MIMO network	174
7.9	Performance comparison of various ANN structures for 2 hidden layers MIMO network	175
7.10	Operating parameters bound used in multi-responses optimization of DBD plasma reactor without catalyst	183
7.11	Computational parameters of Genetic Algorithm used in the multi-responses optimization	183
7.12	Experimental data of hybrid catalytic DBD plasma reactor at low temperature	191
7.13	Operating parameters bound used in multi-responses optimization of catalytic DBD plasma reactor	203
7.14	Computational parameters of Genetic Algorithm used in the multi-responses optimization	204
7.15	Comparison between plasma and conventional fixed bed reactors at the same catalyst (12.8CaO-6.4MnO/CeO_2) and total feed flow rate	210

LIST OF FIGURES

FIGURE NO.	TITLE	PAGE
1.1	Various direct and indirect routes for the production of useful chemicals from natural gas	3
1.2	Ethylene feedstocks in the United States (in billion pounds)	4
1.3	Energy activation of a reaction along the reaction coordinate	12
2.1	Flow chart of general research methodology	25
2.2	Flow chart of comprehensive catalysts screening method	26
2.3	Flow chart of detailed single- and multi-responses optimizations method	27
2.4	Impregnation method for preparing binary metal oxides catalysts	28
2.5	Impregnation method for preparing ternary metal oxides catalysts	29
2.6	Schematic of experimental rig setup for catalyst testing: (1) Ball valve (Swagelok); (2) Volumetric Flow Controllers (Alicat Scientific, Inc.); (3) One-way valve (Swagelok); (4) 4-way Plug valve (Swagelok); (5) 3-way plug valve (Swagelok); (6) Tube Furnace (Carbolite); (7) Quartz tube reactor; (8) Catalyst zone; (9) Controller for furnace; (10) Thermocouple; (11) Condenser (water trap); (12) Online Gas Chromatography-TCD (Agilent 6890); (13) Computer (HP)	35
2.7	Schematic of catalytic quartz fixed bed reactor. (1) catalyst; (2) quartz wool; (3) quartz tube; (4) Teflon ferrule; (5) stainless steel tube (Swagelok); (6) adapter and fitting	36

FIGURE NO.	TITLE	PAGE
2.8	Schematic of temperature program for GC-TCD Agilent 6890	38
2.9	Schematic diagram for experimental rig set-up of DBD plasma reactor: (1). Ball valve; (2). Volumetric flow controller; (3). Check valve; (4,5). Four and three way valves; (6). DBD plasma reactor; (7). High voltage probe; (8). DC power supply; (9). High voltage AC generator; (10). Oscilloscope; (11). Condensor; (12). Online GC; (13). Computer for GC; (P). Pressure gage	42
2.10	Schematic diagram of DBD plasma reactor	43
2.11	Photograph of integrated experimental DBD plasma reactor: (a). Experimental rig set-up; (b). DBD plasma reactor	44
2.12	Schematic diagram of catalytic DBD plasma reactor	45
2.13	Scheme of high voltage generator circuit	45
3.1	Effect of temperature on equilibrium mole fractions presented at 1 atm and: (a) CO_2/CH_4=1/2; (b) CO_2/CH_4=1; (c) CO_2/CH_4=2	59
3.2	Effect of temperature on equilibrium CH_4 and CO_2 conversions presented at 1 atm and: (a) CO_2/CH_4=1; (b) CO_2/CH_4=2	60
3.3	Effect of temperature on equilibrium selectivities of H_2, CO, C_2H_6 and C_2H_4 products presented at 1 atm and: (a) CO_2/CH_4=1; (b) CO_2/CH_4=2	61
3.4	Effect of temperature on equilibrium yields of H_2, CO, C_2H_6 and C_2H_4 products presented at 1 atm and: (a) CO_2/CH_4=1; (b) CO_2/CH_4=2	62
3.5	Effect of system pressure on equilibrium mole fractions of products presented at CO_2/CH_4 feed ratio 1. (a) CH_4, CO_2, CO, H_2O and H_2 at temperature 1123 K, (b) C_2H_6 and C_2H_4 at temperature 923, 1123 and 1223 K	67

FIGURE NO.	TITLE	PAGE
3.6	Effect of system pressure on equilibrium selectivities of H_2, CO, C_2H_6 and C_2H_4 products presented at temperature 1123 K and CO_2/CH_4 feed ratio 1	67
3.7	Effect of system pressure on equilibrium conversions of CH_4 and CO_2 presented at temperature 1123 K and CO_2/CH_4 feed ratio 1	68
3.8	Carbon and no carbon formations region at 1 atm as function of temperature and CO_2/CH_4 feed ratio	69
4.1	Raman spectra of the fresh CeO_2, MnO/CeO_2 and $MnO/CaO/CeO_2$ catalysts. (a) CeO_2 (fresh); (b) 5 wt.% MnO/CeO_2 (fresh); (c) 5 wt.% MnO/15 wt.% CaO/CeO_2	75
4.2	FT-IR spectra of CeO_2, MnO/CeO_2 and $MnO/CaO/CeO_2$ catalysts. (a) CeO_2; (b) 5 wt.% MnO/CeO_2; (c) 5 wt.% MnO/15 wt.% CaO/CeO_2	76
4.3	Raman spectra of the fresh CeO_2, CaO/CeO_2 and $WO_3/CaO/CeO_2$ catalysts. (a) CeO_2 (fresh); (b) 15 wt.% CaO/CeO_2 (fresh); (c) 3 wt.% WO_3/15 wt.% CaO/CeO_2 (fresh)	78
4.4	FT-IR spectra of CeO_2, CaO/CeO_2 and $WO_3/CaO/CeO_2$ catalysts. (a) CeO_2; (b) 15 wt.% CaO/CeO_2; (c) 3 wt.% WO_3/15 wt.% CaO/CeO_2	79
4.5	Stability test of 5 wt.% MnO/15 wt.% CaO/CeO_2 in CO_2 OCM process	80
5.1	X-ray diffraction patterns of fresh CeO_2-based catalysts. (a) CeO_2; (b) 12.8CaO/CeO_2; (c) 12.8CaO-6.4MnO/CeO_2	84
5.2	CO_2-TPD spectra of different fresh catalysts. (a) CeO_2; (b) 12.8CaO/CeO_2; (c) 12.8CaO-6.4MnO/CeO_2	85
5.3	H_2-TPR spectra of different catalysts. (a) CeO_2 (fresh); (b) 12.8CaO/CeO_2 (fresh); (c) 12.8CaO-6.4MnO/CeO_2 (fresh); (d) 12.8CaO-6.4MnO/CeO_2 (used)	90

FIGURE NO.	TITLE	PAGE
6.1	Technique for solving multi-responses optimization problem. (a) mapping from parameter space (Ω) into objective function space (Λ); (b) set of non-inferior solutions or Pareto-optimal solutions	105
6.2	Surface plot of CH_4 conversion as function of reactor temperature and CO_2/CH_4 ratio depicted at fixed catalyst compositions	114
6.3	Contour plot of CH_4 conversion as function of wt.% MnO and wt.% CaO shown at fixed process parameters	115
6.4	Surface plot of C_2 selectivity as function of reactor temperature and CO_2/CH_4 ratio depicted at fixed catalyst compositions	119
6.5	Contour plot of C_2 selectivity as function of wt.% MnO and wt.% CaO in the catalyst presented at fixed process parameters	120
6.6	Contour plot of C_2 yield as function of reactor temperature and wt.% CaO in the catalyst presented at fixed CO_2/CH_4 ratio and wt.% MnO in the catalyst	124
6.7	Contour plot of C_2 yield as function of reactor temperature and wt.% MnO in the catalyst depicted at fixed CO_2/CH_4 ratio and wt.% CaO in the catalyst	124
6.8	Surface plot of C_2 yield as function of reactor temperature and CO_2/CH_4 ratio depicted at fixed catalyst compositions	125
6.9	Relation of weighting factors variation and objective functions (C_2 selectivity and yield) in Pareto-optimal solutions	128
6.10	Relation of weighting factors variation and objective functions (CH_4 conversion and C_2 selectivity) in Pareto-optimal solutions	129
6.11	Relation of weighting factors variation and objective functions (CH_4 conversion and C_2 yield) in Pareto-optimal solutions	130

FIGURE NO.	TITLE	PAGE
6.12	Pareto-optimal solution for multi-responses optimization of C_2 selectivity and yield in CO_2 OCM process	131
6.13	Pareto-optimal solution for multi-responses optimization of CH_4 conversion and C_2 selectivity in CO_2 OCM process	132
6.14	Pareto-optimal solution for multi-responses optimization of CH_4 conversion and C_2 yield in CO_2 OCM process	132
6.15	Location of final optimal conditions for simultaneous C_2 selectivity and yield optimization using maximum normalized $\Sigma\hat{\boldsymbol{F}}(\boldsymbol{X})$ as criterion from Pareto-optimal solution	134
6.16	Location of final optimal conditions for simultaneous CH_4 conversion and C_2 selectivity optimization using maximum normalized $\Sigma\hat{\boldsymbol{F}}(\boldsymbol{X})$ as criterion from Pareto-optimal solution	134
6.17	Location of final optimal conditions for simultaneous CH_4 conversion and C_2 yield optimization using maximum normalized $\Sigma\hat{\boldsymbol{F}}(\boldsymbol{X})$ as criterion from Pareto-optimal solution	135
7.1	Basic configurations of dielectric-barrier discharge	146
7.2	Principles of ANN algorithm	153
7.3	A schematic diagram of the multi-layered perceptron (MLP) in feedforward neural network with backpropagation training	155
7.4	Flowchart of the hybrid ANN-GA algorithms for modelling and optimization	165
7.5	Voltage waveform of pulse AC high voltage power supply	169
7.6	Plasma discharge resulted by high voltage and methane-carbon dioxide based gases	170
7.7	Comparison of predicted and observed values of the 3-9-11-4 ANN model of DBD plasma without catalyst for the following outputs: (a) CH_4 conversion (Y_1), (b) C_{2+} selectivity (Y_2), (c) H_2 selectivity (Y_3), (d) C_{2+} yield (Y_4)	176

FIGURE NO.	TITLE	PAGE
7.8	Dynamic of means square error (MSE) during training and test of the ANN model	177
7.9	Effect of CH_4/CO_2 feed ratio on DBD plasma reactor performance without catalyst at discharge voltage 15 kV and 25 cm^3/min total feed flow rate: CH_4 conversion, C_{2+} selectivity, H_2 selectivity, C_{2+} yield	179
7.10	Effect of discharge voltage on DBD plasma reactor performance without catalyst at CH_4/CO_2 feed ratio 2.5 and 25 cm^3/min total feed flow rate: CH_4 conversion, C_{2+} selectivity, H_2 selectivity, C_{2+} yield	181
7.11	Effect of total feed flow rate on DBD plasma reactor performance without catalyst at CH_4/CO_2 feed ratio 2.5 and discharge voltage 15 kV: CH_4 conversion, C_{2+} selectivity, H_2 selectivity, C_{2+} yield	181
7.12	The dynamics of fitness value and best individual during multi-responses optimization using Genetic Algorithm (GA)	185
7.13	Pareto optimal solutions obtained from the Case 1 (simultaneous maximization of CH_4 conversion (Y_1) and C_{2+} selectivity (Y_2))	185
7.14	Operating parameters corresponding to the Pareto optimal solutions of simultaneous maximization of CH_4 conversion (Y_1) and C_{2+} selectivity (Y_2). X_1: CH_4/CO_2 feed ratio, X_2: discharge voltage (kV), X_3: total feed flow rate (cm^3/min)	186
7.15	Pareto optimal solutions obtained from Case 2 (simultaneous maximization of CH_4 conversion (Y_1) and C_{2+} yield (Y_2))	187

FIGURE NO.	TITLE	PAGE
7.16	Operating parameters corresponding to the Pareto optimal solutions of simultaneous maximization of CH_4 conversion (Y_1) and C_{2+} yield (Y_2). X_1: CH_4/CO_2 feed ratio, X_2: discharge voltage (kV), X_3: total feed flow rate (cm^3/min)	187
7.17	Pareto optimal solutions obtained from the Case 3 (simultaneous maximization of CH_4 conversion (Y_1) and H_2 selectivity (Y_2))	189
7.18	Operating parameters corresponding to the Pareto optimal solutions of simultaneous maximization of CH_4 conversion (Y_1) and H_2 selectivity (Y_2). X_1: CH_4/CO_2 feed ratio, X_2: discharge voltage (kV), X_3: total feed flow rate (cm^3/min)	189
7.19	Comparison of predicted and observed values of the 4-9-11-5 ANN model of catalytic DBD plasma process for the following outputs: (a) CH_4 conversion (Y_1), (b) C_{2+} selectivity (Y_2), (c) H_2 selectivity (Y_3), (d) C_{2+} yield (Y_5), (e) H_2/CO ratio (Y_5)	192
7.20	Dynamic of mean square error (MSE) during training and test of the 4-9-11-5 ANN model of catalytic DBD plasma process	193
7.21	Effect of CH_4/CO_2 feed ratio on catalytic DBD plasma reactor performance at discharge voltage 15 kV, 30 cm^3/min total feed flow rate and reactor temperature 473 K. CH_4 conversion, C_{2+} selectivity, H_2 selectivity, C_{2+} yield, H_2/CO ratio	197
7.22	Effect of discharge voltage on catalytic DBD plasma reactor performance at CH_4/CO_2 feed ratio 2.5, 30 cm^3/min total feed flow rate and reactor temperature 473 K. CH_4 conversion, C_{2+} selectivity, H_2 selectivity, C_{2+} yield, H_2/CO ratio	198

FIGURE NO.	TITLE	PAGE
7.23	Effect of total feed flow rate on catalytic DBD plasma reactor performance at CH_4/CO_2 feed ratio 2.5, discharge voltage 15 kV and reactor temperature 473 K. CH_4 conversion, C_{2+} selectivity, H_2 selectivity, C_{2+} yield, H_2/CO ratio	199
7.24	Effect of reactor wall temperature on catalytic DBD plasma reactor performance at CH_4/CO_2 feed ratio 2.5, discharge voltage 15 kV and total feed flow rate 30 cm^3/min. CH_4 conversion, C_{2+} selectivity, H_2 selectivity, C_{2+} yield, H_2/CO ratio	200
7.25	Pareto optimal solutions obtained from simultaneous maximization of CH4 conversion (Y_1) and C_{2+} selectivity (Y_2) (Case 1) for catalytic DBD plasma reactor	204
7.26	Operating parameters corresponding to the Pareto optimal solutions of simultaneous maximization of CH_4 conversion (Y_1) and C_{2+} selectivity (Y_2) for catalytic DBD plasma reactor. X_1: CH_4/CO_2 feed ratio, X_2: discharge voltage (kV), X_3: total feed flow rate (cm^3/min), X_4: reactor wall temperature (K)	205
7.27	Pareto optimal solutions obtained from simultaneous maximization of CH_4 conversion (Y_1) and C_{2+} yield (Y_2) (Case 2) for catalytic DBD plasma reactor	206
7.28	Operating parameters corresponding to the Pareto optimal solutions of simultaneous maximization of CH_4 conversion (Y_1) and C_{2+} yield (Y_2) for catalytic DBD plasma reactor. X_1: CH_4/CO_2 feed ratio, X_2: discharge voltage (kV), X_3: total feed flow rate (cm^3/min), X_4: reactor wall temperature (K)	207
7.29	Pareto optimal solutions obtained from simultaneous maximization of H_2 selectivity (Y_1) and H_2/CO ratio (Y_2) (Case 3) for catalytic DBD plasma reactor	208

FIGURE NO.	TITLE	PAGE
7.30	Operating parameters corresponding to the Pareto optimal solutions of simultaneous maximization of H_2 selectivity (Y_1) and H_2/CO ratio (Y_2) for catalytic DBD plasma reactor. X_1: CH_4/CO_2 feed ratio, X_2: discharge voltage (kV), X_3: total feed flow rate (cm^3/min), X_4: reactor wall temperature (K)	208

LIST OF ABBREVIATIONS

O_2 OCM	-	Oxygen Oxidative Coupling of Methane
CO_2 OCM	-	Carbon Dioxide Oxidative Coupling of Methane
syngas	-	Synthesis Gas
CORM	-	Carbon Dioxide Reforming of Methane
RWGS	-	Reverse Water Gas Shift
XRD	-	X-ray Diffraction
FT-IR	-	Fourier Transform Infra Red
CO_2-TPD	-	CO_2 Temperature Programmed Desorption
H_2-TPR	-	H_2 Temperature Programmed Reduction
DBD	-	Dielectric Barrier Discharge
WSSOF	-	Weighted Sum of Squared Objective Function
ANN	-	Artificial Neural Network
GA	-	Genetic Algorithm
CCD	-	Central Composite Design
RSM	-	Response Surface Methodology
S	-	Catalyst Support
M_1O	-	First metal oxide in ternary metal oxide
M_2O	-	Second metal oxide in ternary metal oxide
M_aO	-	Metal oxide in binary metal oxide
TCD	-	Thermal Conductivity Detector
PRSS	-	Petronas Research & Scientific Services
HP	-	Hewlet Packard
GC	-	Gas Chromatography
RT	-	Retention Time
MTG	-	Methanol to Gasoline
NSGA	-	Non-dominated Sorting Genetic Algorithm

CCRD	-	Central Composite Rotatable Design
ANOVA	-	Analysis of Variance
GHSV	-	Gas Hourly Space Velocity
MLP	-	Multi-Layered Perceptron
MSE	-	Mean Square Error
MIMO	-	Multi Input and Multi Output

LIST OF SYMBOLS

b	-	Instrument peak broadening
$\boldsymbol{b}$	-	Network bias parameters for hidden and output layers of the network
$\boldsymbol{b}^H$	-	Scalar bias corresponding to hidden layer
b_j	-	Total population in moles of the *j*th atom in the system
$\boldsymbol{b}^O$	-	Scalar bias corresponding to output layer
C	-	Dielectric capacity
d	-	Distance between parallel-plate electrodes
$\hat{\boldsymbol{F}}_{\boldsymbol{i}}$	-	Normalized response/objective function *i*
$\hat{f}_i$	-	Fugacity of species *i* in solution
f_i°	-	Fugacity of pure species *i* in its standard state
$\boldsymbol{F} \in \mathfrak{R}^{\mathbf{M}}$	-	Mapped objectives function space
$F(X)$	-	Multi-response objectives function
$f(\boldsymbol{X})$	-	Single-response objective function
f_1, f_2	-	Nonlinear activation/transfer functions
F_i	-	Inverted objective functions for minimization problem
$F_{i,o}$	-	Real objective functions for minimization problem
$\overline{g}_i$	-	Partial molar Gibbs free energy of the *i*th species in solution
g_i°	-	Gibbs free energy of the pure *i*th species at standard conditions
ΔG_T^o	-	Standard Gibbs free energy changes at temperature T
ΔH_0^o	-	Heat of reaction at reference temperature
ΔG_0^o	-	Gibbs free energy changes at reference temperature
ΔC_p^o	-	Standard heat capacity change of reaction
G	-	Total Gibbs free energy

Gen	-	Generation index
Gen_{max}	-	Maximum generation in Genetic Algorithm
$G_i(\boldsymbol{X})$	-	ith equality constraints
$H_j(\boldsymbol{X})$	-	jth inequality constraints
I	-	Electric current
K	-	Equilibrium constant
k	-	Number of factor
MSE	-	Mean-Squared Error
n	-	Order of the reflection
N	-	Total number of moles in the reaction mixture
n_c	-	Number of points in the cube portion of central composite design
N_i	-	Mole of each chemical species i
n_{ji}	-	Number of the jth atoms that appear in the ith molecule
N_p	-	Number of patterns node used in the training
N_{pop}	-	Number of population
$nvars$	-	Number of independent variables in Genetic Algorithm
P	-	System pressure
P	-	Electric power
P_{cross}	-	Crossover fraction
P^o	-	Standard pressure
Q	-	Charge
R	-	Universal gas constant
R^2	-	Determination coefficient
S	-	Area of electrode
$S(i)$	-	Selectivity of species i
T	-	System temperature
t	-	Time
T_0	-	Reference temperature
$t_{i,k}$	-	Desired (target) value of the kth output node at ith input pattern
V	-	Input voltage
$\boldsymbol{W}$	-	Weighted input
$\boldsymbol{W}$	-	Network weight parameters for hidden and output layers of the network

$\boldsymbol{W}^H$	-	Weights between input and hidden nodes
w_i	-	Weighting factor of objective function *i*
$\boldsymbol{W}^O$	-	Weights between hidden and output nodes
$\boldsymbol{X}\in\mathfrak{R}^{\mathbf{N}}$	-	Parameter space
$X(i)$	-	Conversion of species *i*
$\boldsymbol{x}^*$	-	Optimized population or decision variable vector
X_i, x_i	-	Uncoded and coded independent variables, respectively
$Y(i)$	-	Yield of species *i*
$\boldsymbol{y}^H$	-	Outputs vector from hidden layer
y_i	-	Mole fraction of the *i*th species
$y_{i,k}$	-	Predicted values of the *k*th output node at *i*th input pattern
$\boldsymbol{y}^O$	-	Outputs vector from output layer
α	-	Star point in central composite design
β_o	-	Intercept coefficient in RSM model
β_j	-	Linear terms in RSM model
β_{jj}	-	Squared terms in RSM model
β_{ij}	-	Interaction terms in RSM model
ε	-	Permittivity of dielectric
Σ	-	Summation of data
λ	-	Wavelength of the X-radiation (=0.154 nm)
$\hat{\phi}_i$	-	Fugacity coefficient of the *i*th species in solution
$\boldsymbol{\Omega}$	-	Feasible region
$\boldsymbol{\Lambda}$	-	Mapped feasible region
θ	-	Diffraction angle
ν	-	Stoichiometric number of reaction
ν_i	-	Stoichiometric coefficient of species *i* in reaction

LIST OF APPENDICES

APPENDIX	TITLE	PAGE
A	List of Scientific Publications	232
B	Examples of Performance Calculation using Gas Chromatography Peaks	241
C	MATLAB Program for ΔG_T^o Calculation in Thermodynamic Studies	249
D	MATLAB Program for WSSOF Algorithm for Multi-Response Optimization	252
E	MATLAB Program for Hybrid Artificial Neural Network – Genetic Algorithm (ANN-GA) for Multi-Response Optimization in Dielectric Barrier Discharge Plasma Reactor	266
F	CHEMKIN Graphical User Interface for Thermodynamic Equilibrium Analysis	277

CHAPTER 1

INTRODUCTION

1.1 Methane and Carbon Dioxide Utilization

Natural gas is an abundant fossil fuel resource found all over the world. Though amounts of other gases, such as ethane, propane, H_2S and CO_2, may be present, methane (CH_4) is the main component of the natural gas. The composition of the natural gas is dependent on the location from where it is produced as listed in Table 1.1. Carbon dioxide (CO_2) is one of the most important greenhouse gases. Mitigation of CO_2 emission from various sources has been a worldwide objective. The emission contains particularly about 83% of carbon dioxide, 9% of methane, 6% of nitrous oxide and 2% of hydrofluorocarbons, perfluorocarbons and sulphur hexafluoride (Song, 2001). It has been recognized that enhanced capacities in the area of chemical catalysis could have a significant role in addressing the global atmospheric CO_2 problem. The utilization of CO_2 gas to produce more valuable chemicals is very attractive.

Most of natural gases are located in remote areas, which require a proper infrastructure to transport the gas. As shown in Table 1.1, Malaysia has about 85.8 trillion standard cubic feet of natural gas and ranks as the 11th world's largest natural gas reserve (Sarmidi *et al*., 2001). Therefore, on-site conversion of natural gas into higher valuable products brings out the advantages economically. Another resources as presented in Table 1.2 natural gas from Natuna's and Arun's fields in Indonesia contains CO_2 and CH_4 with CO_2/CH_4 ratio of 71/28 and 15/75, respectively ((Suhartanto *et al.*, 2001; Centi *et al*., 2001). The highly CO_2/CH_4 ratio is potential

to produce higher hydrocarbon, oxygenates and more valuable chemical. A new technology for utilization of carbon dioxide and methane gases is very challenging.

Table 1.1: Gas reserves in Malaysia (Ministry of Energy, Communication, and Multimedia Malaysia, 1999)

Region	Trillion standard cubic feet
Peninsular Malaysia	34.4
Sabah	43.7
Sarawak	7.7
Total	85.8

Table 1.2: Composition of natural gas (in % vol.) from various locations

Component	Terengganu (Malaysia) [1)]	Natuna (Indonesia) [2)]	Terrell County (Texas USA) [3)]	Arun (Indonesia) [4)]
Methane (CH_4)	80.93	28.0[a]	45.7	75
Ethane (C_2H_6)	5.54	-	0.2	5.5
Propane (C_3H_8)	2.96	-	-	3.4[b]
Butane (C_4H_{10})	1.40	-	-	-
>=C_{5+}	-	-	-	0.8
Nitrogen (N_2)	0.10	0.5	0.2	0.3
Carbon dioxide (CO_2)	8.48	71.0	53.9	15
Hidrogen Sulfida (H_2S)	-	0.5	-	0.01

[a] CH_4 + low C_{2+} hydrocarbons
[b] C_3, C_4 hydrocarbons
[1)] Gordon et al. (2001)
[2)] Suhartanto *et al.* (2001)
[3)] Bitter (1997)
[4)] Centi *et al*. (2001)

Conversion of methane and carbon dioxide is important subject in the field of C_1 chemistry. Several technologies have been proposed to improve the efficiency of energy conversion and utilization of CO_2. Alternatively, the recovered CO_2 can be used to produce high value-added chemicals, fuels and other useful products. There are several motivations for producing chemicals from CO_2 whenever possible: (1) CO_2 is an inexpensive, non-toxic feedstock, (2) CO_2 is a renewable feedstock compared to oil or coal, (3) the production of chemicals from CO_2 can lead to new

materials such as polymers, (4) new routes to existing chemical intermediates and products could be more efficient and economical than existing method, (5) The production of chemicals from CO_2 could have a small but significant positive impact on the global carbon balance.

Up to recently, methane conversion has been developed into C_2 hydrocarbons via oxidative coupling of methane with oxygen as an oxidant, known as O_2 OCM hereafter, (Krylov and Mamedov, 1995; Al-Zahrani, 2001; Wolf, 1992) or carbon dioxide as an oxidant, known as CO_2 OCM hereafter, (Asami *et al*., 1995, 1997; Wang and Ohtsuka, 2000; Jiang *et al*., 2002), single step conversion to liquid fuels with oxygen (Eliasson *et al*., 2000; Huang *et al*., 2001b) or partially oxidized to methanol or formaldehyde (Lu *et al*., 1996). Another challenge of the natural gas processing is to convert it into more valuable products indirectly via synthesis gas formation via partial oxidation, steam reforming or CO_2 reforming of methane (Davis, 2001; Kulawska and Skrzypek, 2001; Raje *et al*., 1997; Gesser and Hunter, 1998; Froment, 2000; Wilhelm *et al*., 2001). The various direct and indirect routes for the production of useful chemicals from natural gas are depicted in Figure 1.1 (Ross *et al*., 1996).

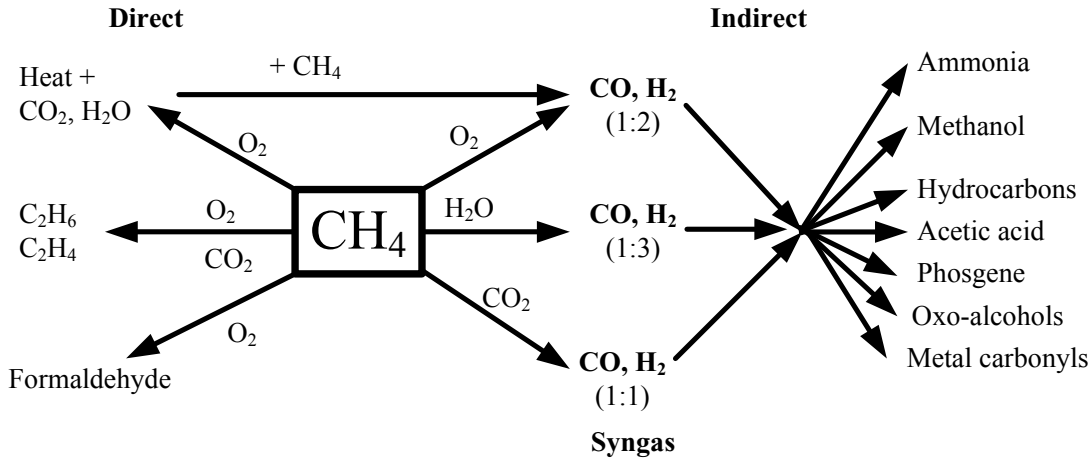

Figure 1.1 Various direct and indirect routes for the production of useful chemicals from natural gas

The C_2 hydrocarbons involve acetylene, ethylene and ethane, where ethane is primary used for the formation of ethylene by dehydrogenation, and ethylene has largely replaced acetylene as a petrochemical source. The United States alone produces nearly 60 billion pounds of ethylene per year (Gordon *et al*., 2001). Ethylene is highly reactive, due to its double bond, allowing it to be converted to a large variety of products by addition, oxidative and polymerization reactions, such as high and low density polyethylene, ethylene dichloride, ethylene glycol, ethylene oxide, ethylbenzene, vinyl acetate, polyvinyl chloride and polyesters (Kniel *et al*., 1980) and to be oligomerized to liquid hydrocarbons.

Ethylene can be derived from many different feedstocks. Ethylene was originally manufactured by partial hydrogenation of acetylene, dehydration of ethanol, or low temperature decomposition of coke-oven gas (Weissermel and Arpe, 2003). The feedstock and the resulting process vary which is dependent on the region. Figure 1.2 reveals different feedstocks used in the production of ethylene and their relative amounts in United Sates (Gordon *et al*., 2001). However, for Western Europe and Japan naphta is the primary feedstock for the production of ethylene since natural gas is less abundant (Weissermel and Arpe, 2003).

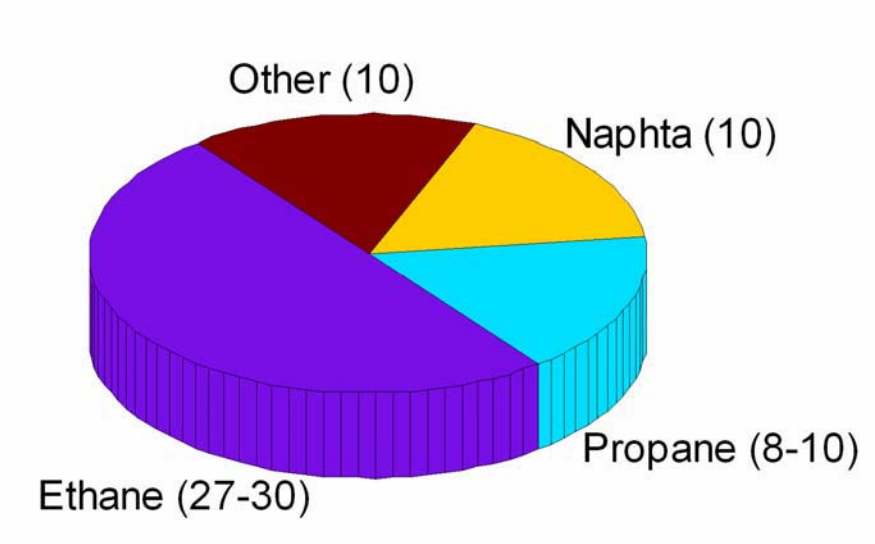

Figure 1.2 Ethylene feedstocks in the United States (in billion pounds) (Gordon *et al*., 2001)

Recently, the thermal cracking of petroleum-based naphta with steam, known as pyrolysis, was used for over 97% of the worldwide production of ethylene. This process uses a feed stream that is a mixture of hydrocarbons and steam. The feed stream is preheated to a temperature of 773-923 K and then raised to 1023-1148 K in controlled manner in a radiant tube (Centi *et al*., 2001). In the radiant tube, the hydrocarbons crack into the major products (ethylene, olefins, and diolefins). Due to the high temperatures required for the endothermic reaction, an intensive energy input is required to drive the process. The production of ethylene from ethane was also done by steam cracking. A typical ethane process operates near 60% conversion of ethane and achieves an ethylene selectivity of 85% (Gordon *et al*., 2001). Over 10% of the ethane is thereby converted into carbon dioxide, and nitrogen oxides are also formed by the combustion. Production of ethylene by steam cracking is a large contributor to the greenhouse gases. It is a challenge to introduce the technologies that will reduce the emission of greenhouse gases during the production of ethylene.

1.1.1 Carbon Dioxide Reforming of Methane

Carbon dioxide reforming converts methane to synthesis gas with low H_2/CO ratio ($H_2/CO \approx 1$). Therefore, the synthesis gas is used for production of liquid hydrocarbon in Fischer-Tropsch synthesis network. Carbon dioxide reforming of methane (CORM) is also known as dry reforming of methane due to the use of CO_2 gas instead of steam. The reaction scheme of CORM is depicted in Equation (1.1).

$$CH_4 + CO_2 \rightleftharpoons 2CO + 2H_2 \quad \Delta H^o_{298} = +247 \text{ kJ/mol} \qquad (1.1)$$

However, simultaneously the H_2 product can react with CO_2 to form CO and H_2O, namely Reverse Water Gas Shift (RWGS) reaction, as depicted in Equation (1.2). The RWGS reaction reduces the H_2 product and causes decrement of H_2/CO ratio.

$$CO_2 + H_2 \rightleftharpoons CO + H_2O \quad \Delta H^o_{298} = +41 \text{ kJ/mol} \qquad (1.2)$$

Among the direct routes, the CORM produces the lowest hydrogen content in the synthesis gas (Ross *et al*., 1996). The CORM is a very reasonable route for the chemical production according to the low H_2/CO ratio that is very effective for further synthesis of valuable oxychemical as reported by Stagg-Williams (1999) and suitable for Fischer-Tropsch process.

1.1.2 Carbon Dioxide Oxidative Coupling of Methane

The oxidative coupling of methane (OCM) is a promising and a novel route for the conversion of methane to C_2 hydrocarbons in the presence of basic catalyst at temperature 923 to 1123 K (Choudhary *et al*., 1999). Several studies have been reported owing to the catalytic OCM using O_2 (O_2 OCM) as an oxidant (Wolf *et al*., 1992; Davydov *et al*., 1995; Barchert and Baerns, 1997; Johnson *et al*., 1997; Zeng *et al*., 2001; Krylov and Mamedov, 1995; Lunsford, 2000) since its high reactivity toward oxidation reaction.

In O_2 OCM, the inevitable formation of CO and CO_2, however, seems to be one of the most serious problems from practical point of view. Recently, carbon dioxide has been used instead of oxygen as an oxidant in CO_2 OCM to produces active oxygen species, which in turn activates methane to CH_3^* radical (Amariglio *et al*., 1998; Nozaki *et al*., 1990; Asami *et al*., 1995,1997; Krylov and Mamedov, 1995; Pareja *et al*., 1998; Wang and Ohtsuka, 2001). Unlike oxygen, CO_2 does not induce gas phase radical reactions (Wang and Ohtsuka, 2001). In other words, the reactions of CH_4 and CO_2 to produce C_2 hydrocarbons are controlled by heterogeneous catalysis. It is thus expected to develop an active catalyst having high selectivity to C_2 hydrocarbons. Equations (1.3) and (1.4) are the two main reaction schemes for CO_2 OCM to produce C_2 hydrocarbons with carbon monoxide and water as the by-products.

$$2CH_4 + CO_2 \rightleftharpoons C_2H_6 + CO + H_2O \quad \Delta H^o_{298} = +106 \text{ kJ/mol} \qquad (1.3)$$

$$2CH_4 + 2CO_2 \rightleftharpoons C_2H_4 + 2CO + 2H_2O \quad \Delta H^o_{298} = +284 \text{ kJ/mol} \qquad (1.4)$$

Moreover, equilibrium conversion of CH_4 to C_2H_6 and C_2H_4 from thermodynamic calculations was studied by Wang *et al*. (1999). The equilibrium conversion increased as the raising temperature and CO_2/CH_4 ratio. High CO_2/CH_4 ratio favours the CH_4 conversion to C_2H_6 and C_2H_4 and their yield exceed 15% and 25%, respectively at 1073 K for CO_2/CH_4 reactant ratio of 2. The key point for realization is to develop an efficient catalyst, which is capable not only for activating both CH_4 and CO_2 but also for producing C_2 hydrocarbons selectively.

1.2 Current Catalyst Technology in CO_2 OCM

Direct methane and carbon dioxide conversion into C_2 hydrocarbons provides a novel route for simultaneous activation and utilization of methane and carbon dioxides. The direct conversion of methane to more valuable chemicals has been an attractive task in catalytic studies by utilizing carbon dioxide as an oxidant. Among several processes, oxidative coupling of methane to ethane and ethylene has been studied most intensively (Asami *et al*., 1995, 1997; Wang *et al*., 1998a, 1998b; Wang *et al*., 1999; Wang and Ohtsuka, 2000, 2001; Jiang *et al*., 2002; Cai *et al*., 2003). The previous studies on CO_2 OCM are summarized in Table 1.3 which is presented historically.

Enhancement of C_2 hydrocarbons formation by CO_2 was first observed in the oxidative coupling of methane over a PbO/MgO catalyst, but it could not be sustained in the absence of O_2 (Wang and Zhu, 2004). Asami *et al*. (1995, 1997) systematically investigated the catalytic activities of more than 30 metal oxides for the conversion of CH_4 by CO_2 in the absence of O_2. They found that lanthanide oxides generally showed higher activities. Among them, praseodymium oxide or terbium oxide exhibited relatively good catalytic performance with a C_2 yield of 1.5% and a selectivity of 50% at 1123 K. Wang *et al*. (1998c) further investigated the conversion of CH_4 to C_2H_6 over praseodymium oxide and reported that the praseodymium oxide could be effective in the presence of CO_2 at temperatures as low as 773 – 923 K to form C_2 hydrocarbons.

In addition to the mono oxide, binary oxide catalysts were also investigated by several research groups for CO_2 OCM as presented in Table 1.3. From Table 1.3, a binary oxide (La_2O_3-ZnO) was observed to have high C_2 hydrocarbons selectivity and good stability, giving a C_2 yield of 2.8% (Chen *et al*., 1996). Although this yield is better than that of any monoxide system reported previously, it is still quite low. Wang *et al*. (1998a, 1998b, 1999) investigated ceria that had been modified with alkali metal and alkaline earth metal oxides for the reaction and reported that CaO-CeO_2 catalyst systems are potential. They suggested that the C_2 yield could reach 6.1% at 1173 K over the CaO-CeO_2 catalyst. Characterization of the system indicated that the redox of Ce^{4+}/Ce^{3+} is responsible for the activation of CO_2, i.e. the dissociation to CO and oxygen species, which accounts for CH_4 conversion, and the basic Ca^{2+} ion in the catalyst greatly enhances the selectivity to C_2 hydrocarbons (Wang *et al*., 1999). In the meantime, they also reported that CaO-Cr_2O_3 catalysts are effective for this reaction (Wang *et al*., 1998b).

Another binary catalyst of CaO-ZnO was also tested by the same group for the reaction (Wang and Ohtsuka, 2001). A C_2 selectivity being 80% and a C_2 yield being 4.3% were achieved over this catalyst with a Ca/Zn ratio of 0.5 at 1148 K. They suggested that the lattice oxygen of the CaO-ZnO catalyst could convert CH_4 mainly to H_2 and CO. The presence of CO_2 contributes to a new oxygen species, which is active and selective for the conversion of CH_4 to C_2 hydrocarbons. The CaO component in the catalyst enhances the adsorption of CO_2 and thus suppresses the reaction involving the lattice oxygen. The reduced-Zn site was suggested to activate CO_2 (Wang and Ohtsuka, 2000).

Table 1.3: Catalyst development for methane oxidative coupling with carbon dioxide to C_2 hydrocarbons

Catalysts	Temperature (K)	CH_4 Conversion (%)	CO_2/CH_4 Ratio	C_2 Hydrocarbons		References
				Selectivity (%)	Yield (%)	
La_2O_3-ZnO	1123	3.1	1.0	91	2.8	Chen *et al.*, 1996
CaO-Cr_2O_3	1123	6.3	2.3	63	4.0	Wang *et al.*, 1998b
CaO-MnO_2	1123	3.9	2.3	68	2.7	Wang *et al.*, 1998b
Na_2WO_4-Mn/SiO_2	1093	4.7	2.0	94	4.5	Liu *et al.*, 1998
CaO-CeO_2	1123	5.0	1.0	62	3.2	Wang *et al.*, 1999
CaO-ZnO	1148	5.4	2.3	80	4.3	Wang and Ohtsuka, 2000
SrO-Cr_2O_3	1123	2.4	2.3	37	1.3	Wang and Ohtsuka, 2001
SrO-ZnO	1123	2.8	2.3	79	2.2	Wang and Ohtsuka, 2001
SrO-CeO_2	1123	1.5	2.3	64	1.0	Wang and Ohtsuka, 2001
SrO-MnO_2	1123	3.9	2.3	85	3.3	Wang and Ohtsuka, 2001
BaO-ZnO	1123	0.6	2.3	74	0.4	Wang and Ohtsuka, 2001
BaO-CeO_2	1123	0.4	2.3	55	0.2	Wang and Ohtsuka, 2001
BaO-Cr_2O_3	1123	0.8	2.3	42	0.3	Wang and Ohtsuka, 2001
BaO-MnO_2	1123	3.8	2.3	67	2.6	Wang and Ohtsuka, 2001
MnO_2-$SrCO_3$	1148	5.7	2.3	51	4.5	Cai *et al.*, 2003
Nano-sized CeO_2-ZnO	1098	5.7	2.0	83.6	4.8	He *et al.*, 2004

Moreover, Wang and Ohtsuka (2001) further reported their investigations of catalytic performance and kinetics over other binary oxides, mainly $CaO\text{-}MnO_2$ (Wang *et al*., 1998b), $SrO\text{-}MnO_2$, and $BaO\text{-}MnO_2$, for the CO_2 OCM process. At temperatures above 1113 K, the $CaO\text{-}MnO_2$ catalyst exhibited a performance similar to that of other calcium-containing binary oxide catalysts ($CaO\text{-}CeO_2$, $CaO\text{-}Cr_2O_3$, and CaO-ZnO). It was reported that C_2 selectivity and yield at 1123 K increased remarkably with increasing partial pressure of CO_2, and apparent activation energies observed over these catalysts were approximately similar (190-220 kJ/mole) (Wang and Ohtsuka, 2001; Wang *et al*., 1998b). When the temperature decreased from 1113 to 1098 K, CH_4 conversion and C_2 selectivity over the $CaO\text{-}MnO_2$ catalyst abruptly decreased and a discontinuous change was also observed in the Arrhenius plots. On the other hand, the $SrO\text{-}MnO_2$ and $BaO\text{-}MnO_2$ catalysts exhibited kinetic features different from the $CaO\text{-}MnO_2$ system, in which the C_2 selectivity at 1123 K changed only slightly with the partial pressure of CO_2. It was also revealed that the activation energies were constant over the entire temperature range examined and notably lowered. From characterization results, a solid solution of $Ca_{0.48}Mn_{0.52}O$ was the main phase for the $CaO\text{-}MnO_2$ catalyst after reaction at 1123 K, whereas, at 1073 K, some Ca^{2+} ions were separated from the solid solution to form $CaCO_3$, which covered the catalyst surface. With the $SrO\text{-}MnO_2$ and $BaO\text{-}MnO_2$ catalysts, $SrCO_3$ and $BaCO_3$ were formed, along with MnO_2 after reaction and the carbonates were suggested to react with MnO_2 to form $SrMnO_{2.5}$ and $BaMnO_{2.5}$ in the conversion process of CH_4 with CO_2 (Wang and Ohtsuka, 2001). Cai *et al*. (2003) further investigated the system of $Mn/SrCO_3$ with a Mn/Sr ratio of 0.1 and 0.2 for the selective conversion of CH_4 to C_2 hydrocarbons using CO_2 as an oxidant and achieved C_2 selectivies of 88% and 79.1% at 1148 K with a C_2 yield of 4.3% and 4.5%, respectively. Recently, He *et al*. (2004) investigated a nano-CeO_2/ZnO catalyst using a novel combination of homogeneous precipitation with micro-emulsion. Their experimental results demonstrated that methane conversion over the nano-CeO_2/ZnO catalyst was higher than that obtained over catalysts prepared by conventional impregnation. They reported that when the content of ZnO was 33%, the methane conversion was 5.73% with C_2 hydrocarbons selectivity of 83.6% at reaction temperature 1098 K. The yield of C_2 hydrocarbons achieved 4.79%. Unfortunately, more coke was formed on the surface of catalysts at higher temperatures. Pertaining to ternary metal oxide catalyst, $Na_2WO_4\text{-}Mn/SiO_2$ catalyst

was further investigated in the conversion of CH_4 with CO_2 to C_2 hydrocarbons (Liu *et al*., 1998). A C_2 yield and selectivity of about 4.5% and 94%, respectively were obtained at 1093 K (Liu *et al*., 1998).

Zhang *et al*. (2002a) recently reported using pulse corona plasma as an activation method and applied it for the reaction of CH_4 and CO_2 over some catalysts. The products were C_2 hydrocarbons and the by-products were CO and H_2. CH_4 conversion and C_2 hydrocarbons yield were affected by the CO_2 concentration in the feed. The CH_4 conversion increased as the CO_2 concentration in the feed increased, while C_2 hydrocarbons yield decreased. The synergism of La_2O_3/γ-Al_2O_3 and plasma gave a CH_4 conversion of 24.9% and C_2 hydrocarbons yield of 18.1% were obtained at a plasma power input of 30 W. The distribution of C_2 hydrocarbons was changed through the use of a Pd-La_2O_3/γ-Al_2O_3 catalyst and the major C_2 product was ethylene. It is noted that the synergetic effect of catalyst and plasma improves the performance of CH_4 and CO_2 conversion to C_2 hydrocarbons.

1.3 Basic Principles of Heterogeneous Catalysis

1.3.1 Concept of Catalysis

A catalyst is a substance that affects the rate of a reaction but not consumed. The catalyst usually changes a reaction rate by promoting a different molecular path (mechanism) for the reaction which gives lower its activation energy. The reaction coordinate to measure the progress along the reaction and pass over the activation energy barrier is depicted schematically in Figure 1.3. The development and use of catalysts is a major part of the constant search for new ways of enhancing product yield and selectivity of chemical reactions. The catalyst can affect both yield and selectivity, because it is possible to obtain an end product by a different pathway (with lower energy barrier). Indeed, a catalyst changes only the rate of a reaction, but it does not affect the equilibrium.

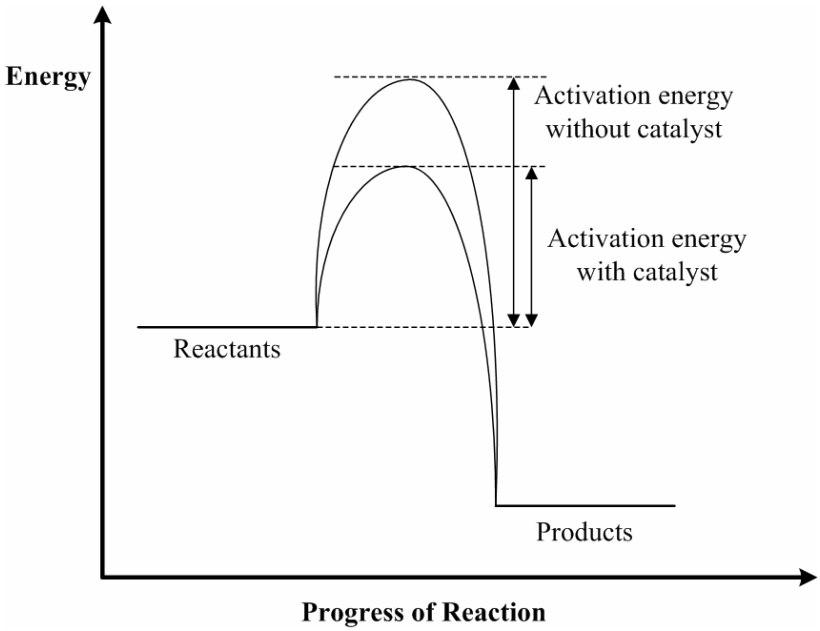

Figure 1.3 Energy activation of a reaction along the reaction coordinate (Fogler, 1999).

Homogeneous catalysis concerns processes in which a catalyst is in solution with at least one of the reactants. A heterogeneous catalytic process involves more than one phase. Usually the catalyst is a solid and the reactants and products are in liquid or gaseous form. The simple and complete separation of the fluid product mixture from the solid catalyst makes heterogeneous catalysis economically attractive. A heterogeneous catalytic reaction occurs at or very near the fluid-solid interface. The principles that govern heterogeneous catalytic reactions can be applied to both catalytic and noncatalytic fluid-solid reactions. There are two other types of heterogeneous reactions involve gas-liquid and gas-liquid-solid system. Reaction between gas and liquid systems are usually mass-transfer limited.

Since a catalytic reaction occurs at fluid-solid interface, a large interfacial area can be helpful or even essential in attaining a significant reaction rate. In many catalysts, this area is provided by a porous structure, where the solid contains many fine pores, and the surface supplies the area needed for the high rate of reaction. The area possessed by some porous materials is surprisingly large. The catalyst that has a large area resulting from pores is called a porous catalyst. Sometimes pores are so small that they will admit small molecules but prevent large ones from entering. Materials with this type of pore are called molecular sieves, and they may be derived

from natural substances such as certain clays and zeolites, or be totally synthetic, such as some crystalline aluminosilicates.

In some cases a catalyst consists of minute particles of an active material dispersed over a less active substance called a support. The active material is frequently a pure metal or metal alloy. Such catalysts are called supported catalysts, as distinguished from unsupported catalysts, whose active ingredients are major amounts of other substances called promoters, which increase the activity.

Pertaining to gas-phase reactions catalyzed by solid surfaces, at least one and frequently all of the reactants must become attached to the surface. This attachment is known as adsorption and takes place by two different processes: physical adsorption and chemisorption. Physical adsorption is similar to condensation, where the process is exothermic and the heat of adsorption is relatively small. The force of attraction between the gas molecules and the solid surface are weak. These van der Waals forces consist of interaction between permanent dipoles, between a permanent dipole and an induced dipole, and/or between neutral atoms and molecules (Centi *et al*., 2001). The amount of gas physically adsorbed decreases rapidly with increasing temperature, and above its critical temperature only very small amounts of a substance are physically adsorbed. The type of adsorption that affects the rate of a chemical reaction is chemisorption. Here, the adsorbed atoms or molecules are held to the surface by valence forces of the same type as those that occurs between bonded atoms in molecules. As a result the electronic structure of the chemisorbed molecule is perturbed significantly, causing it to be extremely reactive. Like physical adsorption, chemisorption is an exothermic process, but the heats of adsorption are generally of the same magnitude as the heat of a chemical reaction. If a catalytic reaction involves chemisorption, it must be carried out within the temperature range where chemisorption of the reactants is appreciable.

A reaction is not catalyzed over the entire solid surface but only at certain active sites or centres. The active sites can also be thought of as places where highly reactive intermediates (chemisorbed species) are stabilized long enough to react. It is defined that an active site as a point on the catalyst surface that can form strong chemical bonds with an adsorbed atom or molecule (Centi *et al*., 2001). One

parameter used to quantify the activity of a catalyst is the turnover frequency. The turnover frequency is the number of molecules reacting per active site per second at the conditions of the experiment. The dispersion of the catalyst is the fraction of the metal atoms deposited that are on the surface. The interaction of reactants with the catalyst surface is a key parameter in heterogeneous reaction systems. For example, the temperature at which species are desorbed from a surface is indicative of the strength of the surface bond where the higher the temperature, the stronger the bond. Therefore the adsorption of a probe molecule at low temperature, and subsequent monitoring of its desorption/reaction characteristics with temperature, is a simply way to characterize surface properties of catalysts and adsorbents.

1.3.2 Point Defects in the Catalyst Structure

Gellings and Bouwmeester (2000) reported an overview study of the defects on catalyst structure. The defects under consideration here may be vacant lattice sites (vacancies), ions placed at normally unoccupied sites (interstitial ions), foreign ions present as impurity or dopant and ions with charges different from those expected from the overall stoichiometry. Electron defects may arise either in the form of ions present with charges deviating from the normal lattice ions, or as a consequence of the transition of electrons from normally filled energy levels, usually the valence band, to normally empty levels, the conduction band. In those cases where an electron is missing, i.e. when there is an electron deficiency, this is usually called an electron hole or hole ($h^{\bullet}$). Usually it is convenient to consider point defects, such as vacancies or electron hole, to be the moving entities in a lattice even though in reality of course the ions or electrons move through the lattice in the opposite direction. The charges of defects and of the regular lattice particles are defined with respect to the neutral, unperturbed (ideal) lattice and are called effective charges. These are indicated by a dot ($^{\bullet}$) for a positive excess charge, by a prime ($'$) for a negative excess charge and by an x (^{x}) for effectively neutral defects (Gellings and Bouwmeester, 2000).

Moreover, Gellings and Bouwmeester (2000) reported on oxidative coupling of methane over CaO-CeO_2 catalysts. With increasing doping of CeO_2 with CaO the concentration of oxygen vacancies and thus of the oxygen ion conductivity increases strongly through the substitution reaction where Ca^{2+} ions are placed on Ce^{4+} sites under formation of Ca''_{Ce} ions, with charge compensation by oxygen vacancies. Kaspar *et al*. (1999) and Terribile *et al*. (1999) suggested that the introduction of relatively small amount of smaller Zr^{4+} or $Mn^{3+}/^{4+}$ into CeO_2 generates defects throughout the matter and brings about an increase of oxygen mobility and pronounces the increasing reducibility of CeO_2.

1.3.3 Role of Acid-Base Properties in Catalytic Oxidation

In addition to the redox properties, transition metal oxides are characterized by the presence of acid-base properties (Centi *et al*., 2001) which also can play a significant role in oxidation reactions. It is thus quite reasonable that in the past many attempts have been made to find correlations between acid-base properties and redox characteristics and catalytic reactivity. The ideal surface structure of an oxide is composed by an array of cations and oxygens, some of which are coordinatively unsaturated and accessible to gas reactants, and thus generate Lewis and Brønsted acidic or basic sites. The strength and number of these sites depend on the nature of the cation, the type of metal to oxygen bond, and the packing of the specific crystalline plane.

The study of the acid-base characteristics and their possible influence on catalytic behaviour is crucial for a better understanding of the surface processes and their control to improve selectivity and reactivity. The acid-base properties of catalyst have three primary roles in relation to the catalytic behaviour (Centi *et al*., 2001): (i) influence on the activation of the hydrocarbons molecule, (ii) influence on the rates of competitive pathways of transformation, and (iii) influence on the rate of adsorption and desorption of reactants and products. Two further ideas may be cited on the topic of the surface reaction mechanisms of selective oxidation:

(1). The combination of acid-base and redox properties of the oxide surface determines the mechanism of transformation

(2). The nature of the oxygen species on the catalyst determines the kind of selectivity.

In the process of oxygen incorporation into the oxide structure, various type of electrophilic activated oxygen species form before being incorporated as structural (lattice) oxygen of the oxide. The latter has a nucleophilic character and gives rise to a different type of attack on an adsorbed alkene and thus different types of products. In the process of incorporation of catalyst structural oxygen into the organic molecule, a point defect forms, which can be compensated for by a change in the linkage of the coordination polyhedra. If the latter process is not a rapid one, and the replenishment of surface oxygen vacancies through oxygen bulk diffusion is also slow, the population of surface electrophilic oxygen species increases with lowering of the selectivity to partial oxidation products. The selectivity is thus a function of the surface geometry of active sites and the redox properties of the catalyst.

1.3.4 Surface Oxygen Species and Their Role in Selective Oxidation

The nature of the surface oxygen species and their reactivity and role in catalysis is obviously a crucial theme in selective oxidation. There are two basic types of oxygen species:

1. Lattice oxygen, which can be either terminal (M=O) or bridging (M-O-M1) oxygen. Further difference arises not only from the strength of these metal-oxygen bonds, which depends on the nature and valence state of the transition metal but also from the coordination of the metal-oxygen polyhedra.
2. Adsorbed radical-type oxygen, formed in the process of the reduction of gaseous O_2 to lattice O^{2-} due to electron transfer from the metal to the oxygen. These species are stabilized by coordination with surface metal ions. During this transformation the nature of the metal-oxygen bond and its polarizability change from an electrophilic character for the negatively charged species to a nucleophilic character for structural O^{2-}.

In general, the reactivity of adsorbed oxygen species has been studied for simple once-through reactions, in which the oxygen species are consumed but no renewed. Oxygen can be involved in oxidation reactions in at least three distinct ways, more than one of which may be operative in any reaction mechanism. The first is the abstraction of a hydrogen from an adsorbed organic molecule to give a radical or carbanion on the surface. The second is the attack on the organic species by a negatively charged oxygen ion whether lattice oxygen or adsorbed oxygen, and the third is the replenishment of lattice oxygen that has been used in a direct oxidation reaction. There are a number of oxygen species: O_2 (adsorbed molecule), O (adsorbed neutral atom), O_2^- (superoxide), O_2^{2-} (peroxide), O_3^- (ozonide), O^-, etc. which may be present on the catalyst surface (Gellings and Bouwmeester, 2000).

A highly basic catalyst is believed to enhance carbon dioxide adsorption, which is then activated on oxygen vacancies to form oxygen active species and gaseous carbon monoxide according to Equations (1.5) and (1.6) using the Kröger-Vink notation (Gellings and Bouwmeester, 2000).

$$V_o^{\bullet\bullet} + 2CO_{2\ (gas)} \rightleftharpoons 2\,O_o^{\bullet} + 2CO_{(gas)} \tag{1.5}$$

$$V_o^{\bullet\bullet} + 2CO_{2\ (gas)} \rightleftharpoons 2\,O_o^{x} + 2CO_{(gas)} + 2h^{\bullet} \tag{1.6}$$

In the Equations (1.5) and (1.6), $V_o^{\bullet\bullet}$ denotes vacancies which will be occupied by doubly ionized oxygen, $h^{\bullet}$ denotes electron holes, O_o^x denotes oxygen ion on neutral lattice positions and $O_o^{\bullet}$ denotes single ionized oxygen on oxygen vacancies as active oxygen species.

1.3.5 Cerium oxide as a Catalyst for CO_2 OCM

Recently, cerium oxide or ceria (CeO_2) plays significant roles in several catalytic processes. Under various redox conditions, the oxidation state of ceria may vary between +3 and +4. Owing to its nonstoichiometric behaviour, CeO_2 has

proved to be a good promoter for oxygen storage in addition to the stabilization of the metals dispersion (Fornasiero *et al*., 1995). Kaspar et al. (1999) suggested that different cations having ionic radii smaller than Ce^{4+} effectively stabilized the CeO_2 against sintering, while all dopants whose radii are larger than Ce^{4+} significantly stabilize with respect to high temperature calcination which means that thermal stabilization of CeO_2 is enhanced. Insertion of a low-valent ion should enhance the oxygen anion mobility in the CeO_2 and increasing the oxygen storage capacity of these materials (Kaspar *et al*., 1999). Two type of oxygen vacancies are created in the doped ceria: intrinsic and extrinsic. The former is due to the reduction of Ce^{4+} according to the following reaction:

$$2Ce_{Ce}^{x} + O_O \rightarrow 2Ce_{Ce}^{'} + V_O^{\bullet\bullet} + \frac{1}{2}O_2 \tag{1.7}$$

while the latter is created by the insertion of the bi- or tri-valent cation according to the following reactions (M denotes metal):

$$MO \xrightarrow{CeO_2} M_{Ce}^{'} + V_O^{\bullet\bullet} + \frac{1}{2}O_2 \tag{1.8}$$

$$M_2O_3 \xrightarrow{CeO_2} 2M_{Ce}^{'} + 2O_O^{x} + V_O^{\bullet\bullet} + \frac{1}{2}O_2 \tag{1.9}$$

Most researchers concluded that the oxidation/reduction reaction of Ce^{4+}/Ce^{3+} is effective to activate carbon dioxide to form oxygen active species which in turn it activate methane (Wang and Ohtsuka, 2001; Wang *et al*., 1998a, 1998b; Cai *et al*., 2003). The C_2 hydrocarbons selectivity may be contributed by the catalyst basicity or the basic sites distribution. This may be due to enhancement of CO_2 chemisorptions on the basic sites in the catalyst surface. CeO_2 have excellent redox properties owing to the very fast reduction of Ce^{4+}/Ce^{3+}, which is associated to the formation of oxygen vacancies at the surface. The oxygen mobility and reducibility of CeO_2-based catalyst can be enhanced by loading transition metal oxide (MnO or WO_3). The addition of transition metal oxides may increase the oxygen vacancy centres, which may be responsible for CO_2 activation to oxygen active species. This phenomenon is inline with suggestion from Kaspar *et al*. (1999) and Terribile *et al*. (1999) where the introduction of relatively small amount of smaller Zr^{4+} or $Mn^{3+/4+}$ into CeO_2 generates defects and brings about an increase of oxygen mobility and pronounces the increasing reducibility of CeO_2. Leitunburg *et al*. (1997) concluded that reduced ceria has a strong effect on CO_2 adsorption and activation. They

suggested that oxygen vacancies, and particularly those present in the bulk, are the driving force for CO_2 activation with the formation of CO and oxidation of reduced ceria.

1.4 Problem of Research

Oxidative coupling of methane is one of the attractive routes for the conversion of methane to higher hydrocarbons via radical formation. The reaction can be carried out by either reducible or non-reducible metal oxide with a feed of methane where lattice oxygen is used as an oxidant or with a co-feed of oxygen or carbon dioxide. However, oxygen unavoidably induces some gas phase radical reaction which causes low C_2 hydrocarbons yield due to reducing methyl radical. However, almost previous research on the CO_2 OCM still exhibited quite low methane conversion and C_2 hydrocarbons yield (Asami *et al*., 1995, 1997; Wang *et al*., 1998a, 1998b, 1999; Wang and Ohtsuka, 2000, 2001; Cai *et al*., 2003; He *et al.*, 2004). The highest CH_4 conversion of 5.7% at 1123 K suggested that the conventional catalyst systems are not effective in activating CH_4 in CO_2 OCM. Therefore it is a great challenge to develop a new catalyst system or to find a new reaction method for the activation of CH_4 and CO_2 to produce C_2 hydrocarbons. The new catalyst and/or suitable reactor system can enhance the activation of CO_2 and CH_4 in order to improve the catalytic performances.

It is believed that carbon dioxide chemisorption is favoured on alkaline earth metal oxides (CaO) rather than other metal oxides (Tanabe *et al*., 1989). However, a strong basic oxide (i.e. SrO, BaO) will not favour the activation of CH_4 (Choudhary *et al*., 1999) due to the quite amount of carbon dioxide adsorbed which thus blocked the active sites of catalyst. An active oxygen species (O^*) produced from CO_2 activation are important in CO_2 OCM in activation of methane. A synergistic effect of oxidation/reduction mechanism and basicity of the catalyst may have a relationship with the CO_2 activation. The reducibility of CeO_2 catalyst could be enhanced by introduction of manganese oxide (MnO_x), while the catalyst basicity could be controlled by doping CaO. Higher reducibility of catalyst leads to

contribution of oxygen vacancies, which are active sites for CO_2 chemisorption. The plentiful of CO_2-adsorbed on the catalyst surface favours the reaction suppression involving the lattice oxygen and enhances the selective conversion of methane to C_{2+} hydrocarbons. However, when only a few CO_2 is chemisorbed, some lattice oxygen would partially take part in the reaction and convert CH_4 mainly to H_2 and CO leading to low C_2 selectivity.

The optimal catalyst compositions in the CeO_2-supported catalyst and the optimal operating parameters, such as the CO_2/CH_4 ratio and reactor temperature, provide essential information for kinetic studies and for implementing the CO_2 OCM process to an industrial scale. From the fact that only low methane conversion and C_2 yield were addressed in the conventional fixed bed reactor, the modification of the reactor such that the methane and carbon dioxide activation in the catalyst surface could be enhanced is required.

1.5 Objectives of Research

The objectives of research are:

a) To study the feasibility of CO_2 OCM reaction via thermodynamic equilibrium analysis
b) To develop a suitable catalyst for CO_2 OCM process with high methane conversion and high selectivity toward C_2 hydrocarbons formation.
c) To investigate the synergistic effect of basicity and reducibility of the catalyst on catalytic activity of CO_2 OCM.
d) To optimize the catalyst compositions and operating conditions including their interaction effect suitable for the CO_2 OCM process.
e) To develop a high performance reactor system suitable for CO_2 OCM process.

1.6 Scopes of Research

The scopes of research are:

a) Thermodynamic equilibrium analysis is conducted to study the feasibility of all possible CH_4 and CO_2 reactions particularly for CO_2 OCM reaction.
b) Catalyst screening is performed on CeO_2-based catalysts for addressing the promising catalyst of CO_2 OCM process.
c) Catalyst characterizations are conducted on the fresh and/or used catalysts using XRD, FT-IR, Raman, CO_2-TPD, H_2-TPR in order to investigate the surface structure, basicity and reducibility of the catalysts.
d) Testing of the catalyst for CO_2 OCM reaction is carried out in a fixed-bed quartz reactor with the certain ranges of operating conditions at fixed atmospheric pressure.
e) The single- and multi-response optimizations are conducted to obtain the optimal catalyst compositions and operating conditions, which gives highly performance toward CO_2 OCM process.
f) The modification of reactor system is intended to achieve high catalytic performance of CO_2 OCM using a hybrid catalytic- dielectric barrier discharge (DBD) plasma reactor. The plasma reactor is aimed to enhance the methane and carbon dioxide activation at lower gas temperatures.

1.7 Organization of Thesis

The research is targeted on the development of a suitable catalyst and a high performance reactor system for CO_2 OCM process. The optimization of catalyst compositions and operating conditions and their interaction effect are discussed. The reactor modification is designed to improve the methane and carbon dioxide conversions using a hybrid catalytic-plasma reactor concept.

This thesis consists of eight chapters. Chapter 1 presents the background, literature review related to CO_2 OCM and basic principles of catalysis, research problem, objectives and scopes of the thesis. In Chapter 2, the general description of

research methodology and the detail experimental strategy are described. Thermodynamic studies on co-generation of C_2 hydrocarbon and synthesis gas from methane and carbon dioxide using direct minimization Gibbs free energy are presented in Chapter 3. Meanwhile, Chapter 4 introduces catalyst screening of CeO_2-based catalysts to provide suitable catalyst for CO_2 OCM, at which some catalyst characterization methods such as FT-IR and Raman spectroscopies were implemented to confirm the surface structure of metal oxides. In this chapter, the CeO_2-based catalyst was addressed as a promising catalyst for the CO_2 OCM. Some catalyst characterization method, i.e. X-ray Diffraction (XRD), H_2-TPR and CO_2-TPD, were applied to investigate the synergistic effect of catalyst basicity and reducibility toward CO_2 OCM process as presented in Chapter 5. In Chapter 6, the optimization of catalyst compositions and operating conditions for the selected catalyst are clearly explored owing to single- and multi-responses optimizations. Here, a new hybrid numerical algorithm is developed for solving the multi-responses optimization. The reactor modification using a hybrid catalytic-Dielectric Barrier Discharge (DBD) plasma reactor at low temperature is addressed in Chapter 7. Finally, Chapter 8 presents the main conclusions of this thesis and recommendations for future work.

REFERENCES

Ahmad, A.L., Azid, I.A., Yusof, A.R., and Seetharamu, K.N. (2004). Emission Control in Palm Oil Mills using Artificial Neural Network and Genetic Algorithm. *Comp. Chem. Eng.* 28: 2709-2715.

Al-Zahrani, S.M.S. (2001). The Effect of Kinetics, Hydrodynamics and Feed Conditions on Methane Coupling Using Fluidized Bed Reactor. *Catal. Today*. 64**:** 217-225.

Amariglio, H., Belqued, M., Pareja, P. and Amariglio, A. (1998). Oxygen-Free Conversion of Methane to Higher Hydrocarbons through a Dual-Temperature Two-Step Reaction Sequence on Platinum and Ruthenium. *J. Catal.* 177**:** 113-120.

Amin, N.A.S. and Istadi. (2006). Selective Conversion of Methane to C_2 Hydrocarbons using Carbon Dioxide as an Oxidant over CaO-MnO/CeO_2 Catalyst. In *Studies in Surface Science Catalysis*. Amsterdam: Elsevier Science B.V. Paper No. CCR14. In Press

Appel, L.G., Eon, J.G. and Schmal, M. (1998). The CO_2-CeO_2 Interaction and Its Role in the CeO_2 Reactivity. *Catal. Lett*. 56: 199-202.

Asami, K., Fujita, T., Kusakabe, K., Nishiyama, Y. and Ohtsuka, Y. (1995). Conversion of Methane with Carbon Dioxide into C_2 Hydrocarbons over Metal Oxides. *Appl. Catal. A: Gen.* 126: 245-255.

Asami, K., Kusakabe, K., Ashi, N. and Ohtsuka, Y. (1997). Synthesis of Ethane and Ethylene from Methane and Carbon Dioxide over Praseodymium Oxide Catalysts. *Appl. Catal. A: Gen.* 156: 43-56.

Banov, B., Momchilov, A., Massot, M. and Julien, C.M. (2003). Lattice Vibrations of Materials for Lithium Rechargeable Batteries V. Local Structure of $Li_{0.3}MnO_2$. *Mat. Sci. Eng. B: Solid.* 100: 87-92.

Barchert, H. and Baerns, M. (1997). The Effect of Oxygen-Anion Conductivity of Metal Oxide Doped Lanthanum Oxide Catalysts on Hydrocarbon Selectivity in the Oxidative Coupling of Methane. *J. Catal.* 168**:** 315-320.

Bigey, C., Hilaire, L., and Maire, G. (2001). WO_3-CeO_2 and Pd/WO_3-CeO_2 as Potential Catalysts for Reforming Applications: I. Physicochemical Characterization Study. *J. Catal.* 198: 208–222.

Bitter, J. H. (1997). *Platinum Based Bifunctional Catalysts for Carbon Dioxide Reforming of Methane – Activity, Stability and Mechanism*. University of Twente: PhD Thesis.

Boaro, M., Vicario, M., Leitenburg, C.D., Dolcetti, G. and Trovarelli, A. (2003). The Use of Temperature-Programmed and Dynamic/Transient Methods in Catalysis: Characterization of Ceria-Based, Model Three-Way Catalysts. *Catal. Today*. 77: 407-417.

Bothe-Almquist, C.L., Ettireddy, R.P., Bobst, A. and Smirniotis, P.G. (2000). An XRD, XPS, and EPR Study of Li/MgO Catalysts: Case of the Oxidative Methylation of Acetonitrile to Acrylonitrile with CH_4. *J. Catal.* 192: 174-184.

Bowen, W.R., Jones, M.J. and Yousef, H.N.S. (1998). Dynamic Ultrafiltration of Proteins – A Neural Network Approach. *J. Membrane Sci.* 146: 225-235.

Box, G.E.P., Hunter, W.G., Hunter, J.S. (1978). *Statistics for Experimenters: An Introduction to Design, Data Analysis, and Model Building*. New York: John Wiley & Sons.

Cadus, L.E. and Ferretti, O. (2002). Characterization of Mo-MnO Catalyst for Propane Oxidative Dehydrogenation. *Appl. Catal. A: Gen.* 233: 239-253.

Cai, Y., Chou, L., Li, S., Zhang, B. and Zhao, J. (2003). Selective Conversion of Methane to C_2 Hydrocarbons Using Carbon Dioxide over Mn-$SrCO_3$ Catalysts. *Catal. Lett.* 86: 191-195.

Caldwell, T.A., Le, H., Lobban, L.L. and Mallinson, R.G. (2001). Partial Oxidation of Methane to Form Synthesis Gas in a Tubular AC Plasma Reactor. in Spivey, J.J., Iglesia, E. and Fleisch, T.H. Eds. *Studies in Surface Science and Catalysis 136*, Amsterdam: Elsevier Science B.V. 265-270.

Centi, G., Cavani, F., and Trifirò, F. (2001). *Selective Oxidation by Heterogeneous Catalysis*. New York: Kluwer Academic/Plenum Publishers.

Chan, S.H. and Wang, H.M. (2000). Thermodynamic Analysis of Natural-Gas Fuel Processing for Fuel Cell Applications. *Int. J. Hydrogen Energy.* 25: 441-449.

Chan, S.H. and Wang, H.M. (2004). Thermodynamic and Kinetic Modelling of an Autothermal Methanol Reformer. *J. Power Sources*. 126: 8-15.

Chen, C., Xu, Y., Lin, G. and Guo, X. (1996). Oxidative Coupling of Methane by Carbon Dioxide: A Highly C_2 Selective La_2O_3/ZnO Catalyst. *Catal. Lett.* 42: 149-153.

Chen, G. (2002). New Advances in Catalytic Systems for Conversion of CH_4 and CO_2. *J. Nat. Gas Chem.* 11: 109-116.

Chen, Y. and Wach, I.E. (2003). Tantalum Oxide-supported Metal Oxide (Re_2O_7, CrO_3, MoO_3, WO_3, V_2O_5, and Nb_2O_5) Catalysts: Synthesis, Raman Characterization and Chemically Probed by Methanol Oxidation. *J. Catal.* 217: 468-477.

Choudhary, V.R. and Rane, V.H. (1991). Acidity/Basicity of Rare-Earth Oxides and their Catalytic Activity in Oxidative Coupling of Methane to C_2-Hydrocarbons. *J. Catal.* 130: 411-422.

Choudhary, V.R., Mulla, S.A.R. and Uphade, B.S. (1999). Oxidative Coupling of Methane over Alkaline Earth Oxides Deposited on Commercial Support Precoated with Rare Earth Oxides. *Fuel*. 78**:** 427-437.

Chow, T.T., Zhang, G.Q., Lin, Z., and Song, C.L. (2002). Global Optimization of Absorption Chiller System by Genetic Algorithm and Neural Network. *Energy Buildings*. 34: 103-109.

Clarke, G.M., and Kempson, R.E. (1997). *Introduction to the Design and Analysis of Experiments*. London: Arnold.

Cornell, J.A. (1990). *How to Apply Response Surface Methodology*. Wisconsin: American Society for Quality Control.

Craciun, R., Nentwick, B., Hadjivanov, K. and Knözinger, H. (2003). Structure and Redox Properties of MnO_x/Yttrium-Stabilized Zirconia (YSZ) Catalyst and its Used in CO and CH_4 Oxidation. *Appl. Catal. A: Gen.* 243: 67-79.

Davis, B.H. (2001). Fischer-Tropsch Synthesis: Current Mechanism and Futuristic Needs. *Fuel Process. Technol.*. 71**:** 157-166.

Davydov, A.A., Shepotko, M.L. and Budneva, A.A. (1995). Basic Sites On The Oxide Surfaces: Their Effect on the Catalytic Methane Coupling. *Catal. Today*. 24**:** 225-230.

de Faveri, D., Torre, P., Perego, P., Converti, A. (2004). Optimization of Xylitol Recovery by Crystallization from Synthetic Solutions using Response Surface Methodology. *J. Food Eng.* 61: 407-412.

Deb, K. (2001). *Multi-objective Optimization Using Evolutionary Algorithms*. Chichester, UK: John Wiley & Sons.

Demuth, H. and Beale, M. (2005). *Neural Network Toolbox for Use with MATLAB*. Natick, MA: The Mathworks, Inc.

Douvartzides, S.L., Coutelieris, F.A., Demin, A.K. and Tsiakaras, P.E. (2003). Fuel Options for Solid Oxide Fuel Cells: a Thermodynamic Analysis. *AIChE J.* 49: 248-257.

Edgar, T.F., Himmelblau, D.M., Lasdon, L.S. (2001). *Optimization of Chemical Processes*. New York: McGraw-Hill, Inc.

Eliasson, B., and Kogelschatz, U. (1991). Modeling and Applications of Silent Discharges Plasmas. *IEEE Trans. Plasma Sci.* 19:309-323.

Eliasson, B., Liu, C.J. and Kogelschatz, U. (2000). Direct Conversion of Methane and Carbon Dioxide to Higher Hydrocarbons using Catalytic Dielectric-Barrier Discharges with Zeolites. *Ind. Eng. Chem. Res.* 39**:** 1221-1227.

Fincke, J.R., Anderson, R.P., Hyde, T., Detering, B.A., Wright, R., Bewley, R.L., Haggard, D.C., and Swank, W.D. (2002). Plasma Thermal Conversion of Methane to Acetylene. *Plasma Chem. Plasma Proc.* 22: 105-136.

Fissore, D., Barresi, A.A., and Manca, D. (2004). Modelling of Methanol Synthesis in A Network of Forced Unsteady-state Ring Reactor by Artificial Neural Networks for Control Purposes. *Chem. Eng. Sci.* 59: 4033-4041.

Fornasiero, P., Di Monte, R., Ranga Rao, G., Kaspar, J., Meriani, S., Trovarelli, A., and Graziani, M. (1995). Rh-Loaded CeO2-ZrO2 Solid Solutions as Highly Efficient Oxygen Exchangers: Dependence of the Reduction Behaviour and the Oxygen Storage Capacity on the Structural Properties. *J. Catal*. 151: 168-177.

Froment, G.F. (2000). Production of Synthesis gas by Steam – and CO_2 Reforming of Natural Gas. *J. Mol. Catal. A: Chem*. 163**:** 147-156.

Gellings, P.J. and Bouwmeester, H.J.M. (2000). Solid State Aspects of Oxidation Catalysis. *Catal. Today*. 58: 1-53.

Gesser, H.D. and Hunter, N.R. (1998). A Review of C-1 Conversion Chemistry. *Catal. Today*. 42**:** 183-189.

Gordon, C.L., Lobban, L.L. and Mallinson, R.G. (2001). Selective Hydrogenation of Acetylene to Ethylene during The Conversion of Methane in a Catalytic DC Plasma Reactor. In: Pivey, J.J., Iglesia, E. and Fleisch, T.H. Eds. *Studies in Surface Science and Catalysis 136*, Amsterdam: Elsevier Science B.V. 271-276.

Gotić, M., Ivanda, M., Popović, S. and Musić, S. (2000). Synthesis of Tungsten Trioxide Hydrates and Their Structural Properties. *Mat. Sci. Eng. B: Solid*. 77: 193-201.

Guéret, C., Daroux, M., and Billaud, F. (1997). Methane Pyrolysis: Thermodynamics. *Chem. Eng. Sci.* 52: 815-827.

Hagan, M.T. and Menhaj, M. (1994). Training Feedforward Networks with the Marquardt Algorithm. *IEEE Trans. Neural Network.* 5: 989-993.

Hammer, Th., Kappes, Th., Baldauf, M. (2004). Plasma Catalytic Hybrid Processes: Gas Discharge Initiation and Plasma Activation of Catalytic Processes. *Catal. Today*. 89:5-14.

Hattori, T. and Kito, S. (1991). Artificial Intelligence Approach to Catalyst Design. *Catal. Today*. 10: 213-222.

Hattori, T. and Kito, S. (1995). Neural Network as a Tool for Catalyst Development. *Catal. Today*. 23: 347-355.

He, Y., Yang, B., and Cheng, G. (2004). On the Oxidative Coupling of Methane with Carbon Dioxide over CeO_2/ZnO Nanocatalysts. *Catal. Today*. 98: 595-600.

Heintze, M., and Pietruszka, B. (2004). Plasma Catalytic Conversion of Methane into Syngas: The Combined Effect of Discharge Activation and Catalysis. *Catal. Today*. 89: 21-25.

Hou, Z., Kefa, C., and Jianbo, M. (2001). Combining Neural Network and Genetic Algorithms to Optimize Low NO_x Pulverized Coal Combustion. *Fuel*. 80: 2163-2169.

Hou, Z.Y., Dai, Q.L., Wu, X.Q. and Chen, G.T. (1997). Artificial Neural Network Aided Design of Catalyst for Propane Ammoxidation. *Appl. Catal. A: Gen.* 161: 183-190.

Huang, A., Xia, G., Wang, J., Suib, S.L., Hayashi, Y., Matsumoto, H. (2000). CO_2 Reforming of CH_4 by Atmospheric Pressure AC Discharge Plasmas. *J. Catal.* 189:349-359.

Huang, K., Chen, F.Q. and Lü, D.W. (2001a). Artificial Neural Network-Aided Design of a Multi-Component Catalyst for Methane Oxidative Coupling. *Appl. Catal. A: Gen.* 219: 61-68.

Huang, W., Xie, K.C., Wang, J.P., Gao, Z.H. and Zhu, Q.M. (2001b). Possibility of Direct Conversion of CH_4 and CO_2 to High-value Products. *J. Catal.* 201**:** 100-104.

Huang, K., Zhan, X.L., Chen, F.Q., and Lü, D.W. (2003). Catalyst Design for Methane Oxidative Coupling by Using Artificial Neural Network and Hybrid Genetic Algorithm. *Chem. Eng. Sci.* 58: 81-87.

Istadi and Amin, N.A.S. (2004). Screening of MgO- and CeO_2-based Catalysts for Carbon Dioxide Oxidative Coupling of Methane to C_{2+} Hydrocarbons. *J. Nat. Gas Chem.* 13: 23-35.

Istadi and Amin, N.A.S. (2005a). A Hybrid Numerical Approach for Multi-Responses Optimization of Process Parameters and Catalyst Compositions in CO_2 OCM Process over CaO-MnO/CeO_2 Catalyst. *Chem. Eng. J.* 106: 213-227.

Istadi and Amin, N.A.S. (2005b). Optimization of Process Parameters and Catalyst Compositions in CO_2 Oxidative Coupling of Methane over CaO-MnO/CeO_2 Catalyst using Response Surface Methodology. *Fuel Process. Technol.* In Press.

Istadi and Amin, N.A.S. (2005c). A Thermodynamic Analysis of Co-generation of C_2 Hydrocarbons and Synthesis Gases from Methane and Carbon Dioxide by Direct Gibbs Free Energy Minimization. *J. Nat. Gas Chem.* 14: 140-150.

Istadi and Amin, N.A.S. (2006). Co-Generation of Synthesis Gas and C_{2+} Hydrocarbons from Methane and Carbon Dioxide in A Hybrid Catalytic-Plasma Reactor: A Review. *Fuel*. 85: 577-592.

Ito, M., Tagawa, T., Goto, S. (1999). Suppression of Carbonaceous Depositions on Nickel Catalyst for the Carbon Dioxide Reforming of Methane. *Appl. Catal. A: Gen.* 177: 15-23.

Jiang, T., Li, Y., Liu, C., Xu, G., Eliasson, B. and Xue, B. (2002). Plasma Methane Conversion Using Dielectric-Barrier Discharges with Zeolite A. *Catal. Today*. 72**:** 229-235.

Johnson, M.A., Stefanovich, E.V. and Truong, T.N. (1997). An *ab initio* Study on the Oxidative Coupling of Methane over a Lithium-doped MgO Catalyst: Surface Defects and Mechanism. *J. Phys. Chem. B*. 101**:** 3196-3201.

Julien, C.M. and Massot, M. (2003). Lattice Vibrations of Materials for Lithium Rechargeable Batteries I. Lithium Manganese Oxide Spinel. *Mat. Sci. Eng. B: Solid*. 97: 217-230.

Jung, S.H., Park, S.M., Park, S.H., and Kim, S.D. (2004). Surface Modification of Fine Powders by Atmospheric Pressure Plasma in A Circulating Fluidized Bed Reactor. *Ind. Eng. Chem. Res.* 43:5483-5488.

Kang, W.S., Park, J.M., Kim, Y., and Hong, S.H. (2003). Numerical Study on Influences of Barrier Arrangements on Dielectric Barrier Discharge Characteristics. *IEEE Trans. Plasma Sci.* 31:504-510.

Kaspar, J., Fornasiero, P. and Graziani, M. (1999). Use of CeO_2-Based Oxides in the Three-Way Catalysis. *Catal. Today*. 50: 285-298.

Ministry of Energy, Communication, and Multimedia Malaysia (1999). *National Energy Balance Malaysia 1980-1998 and Quarter 1 & 2*. Kuala Lumpur: Kementerian Tenaga, Komunikasi dan Multimedia Malaysia.

Kim, S.S., Lee, H., Na, B.K., and Song, H.K. (2004). Plasma-assisted Reduction of Supported Metal Catalyst using Atmospheric Dielectric-barrier Discharge. *Catal. Today*. 89:193-200.

Kizling, M.B., and Järås, S.G. (1996). A Review of the Use of Plasma Techniques in Catalyst Preparation and Catalytic Reactions. *Appl. Catal. A: Gen.* 147:1-21.

Kniel, L., Winter, O. and Stork, K. (1980). *Ethylene: Keystone to the Petrochemical Industry*. New York: Marcel Dekker.

Ko, D. and Moon, I. (2002). Multiobjective Optimization of Cyclic Adsorption Processes. *Ind. Eng. Chem. Res.* 41: 93-104.

Kogelschatz, U. (2003). Dielectric-barrier Discharges: Their History, Discharge Physics, and Industrial Applications. *Plasma Chem. Plasma Process.* 23: 1-46.

Kraus, M., Eliasson, B., Kogelschatz, U., Wokaun, A. (2001). CO_2 Reforming of Methane by the Combination of Dielectric-Barrier Discharges and Catalysis. *Phys. Chem. Chem. Phys.* 3:294-300

Krokida, M.K. and Kiranoudis, C.T. (2000). Pareto Design of Fluidized Bed Dryers. *Chem. Eng. J.* 79: 1-12.

Krylov, O.V. and Mamedov, A.K. (1995). Heterogeneous Catalytic Reactions of Carbon Dioxide. *Russ. Chem. Rev.* 64(9): 877-900.

Kulawska, M. and Skrzypek, J. (2001). Kinetics of the Synthesis of Higher Aliphatic Alcohols from Syngas over a Modified Methanol Synthesis Catalyst. *Chem. Eng. Process.* 40**:** 33-40.

Kuś, S. and Taniewski, M. (2002). The Effect of Some Impurities on The Basicity of MgO Tested by the Transformation of 2-Butanol and on its Catalytic Performance in Oxidative Coupling of Methane. *Fuel Process. Technol.* 76: 41-49.

Kuś, S., Otremba, M. and Taniewski, M. (2003). The Catalytic Performance in Oxidative Coupling of Methane and the Surface Basicity of La_2O_3, Nd_2O_3, ZrO_2 and Nb_2O. *Fuel*. 82: 1331-1338.

Kuś, S., Otremba, M., Tórz, A. and Taniewski, M. (2002). Further Evidence of Responsibility of Impurities in MgO for Variability in its Basicity and Catalytic Performance in Oxidative Coupling of Methane. *Fuel*. 81: 1755-1760.

Laosiripojana, N. and Assabumrungrat, S. (2005). Catalytic Dry Reforming of Methane over High Surface Area Ceria. *Appl. Catal. B: Env*. 60: 107-116.

Larentis, A.L., de Resende, N.S., Salim, V.M.M. and Pinto J.C. (2001). Modeling and Optimization of the Combined Carbon Dioxide Reforming and Partial Oxidation of Natural Gas. *Appl. Catal. A: Gen.* 215: 211-224.

Larkin, D.W., Zhou, L., Lobban, L.L. and Mallinson, R.G. (2001). Product Selectivity Control and Organic Oxygenate Pathways from Partial Oxidation of Methane in a Silent Electric Discharge Reactor. *Ind. Eng. Chem. Res.* 40: 5496-5506.

Leitenburg, C.D., Trovarelli, A., and Kaspar, J. (1997). A Temperature-Programmed and Transient Kinetic Study of CO_2 Activation and Methanation over CeO_2 Supported Noble Metals. *J. Catal*. 166: 98-107.

Leofanti, G., Tozzola, G., Padovan, M., Petrini, G., Bordiga, S. and Zecchina, A. (1997a). Catalyst Characterization: Characterization Techniques. *Catal. Today*. 34: 307-327.

Leofanti, G., Tozzola, G., Padovan, M., Petrini, G., Bordiga, S. and Zecchina, A. (1997b). Catalyst Characterization: Applications. *Catal. Today*. 34: 329-352.

Li, R., Yamaguchi, Y., Yin, S., Tang, Q., and Sato, Ts. (2004a). Influence of Dielectric Barrier Materials to the Behavior of Dielectric Barrier Discharge Plasma for CO_2 Decomposition. *Solid State Ionics*. 172:235-238.

Li, R., Tang, Q., Yin, S., Yamaguchi, Y., and Sato, Ts. (2004b). Decomposition of Carbon Dioxide by the Dielectric Barrier Discharge (DBD) Plasma Using $Ca_{0.7}Sr_{0.3}TiO_3$ Barrier. *Chem. Lett.* 33:412-413.

Li, M.W., Xu, G.H., Tian, Y.L., Chen, L., and Fu, H.F. (2004c). Carbon Dioxide Reforming of Methane Using DC Corona Discharge Plasma Reaction. *J. Phys. Chem. A*. 108: 1687-1693.

Li, Y., Xu, G.-H, Liu, C.-J., Eliasson, B. and Xue, B.-Z. (2001). Co-generation of Syngas and Higher Hydrocarbons from CO_2 and CH_4 Using Dielectric-Barrier Discharge: Effect of Electrode Materials. *Energy Fuels*. 15: 299-302.

Lieberman, M.A. and Lichtenberg, A.J. (1994). *Principles of Plasma Discharges and Materials Processing*. New York: John Wiley & Sons, Inc.

Liu, C.J., Li, Y., Zhang, Y.P., Wang, Y., Zou, J., Eliasson, B., et al. (2001a). Production of Acetic Acid Directly from Methane and Carbon Dioxide Using Dielectric-Barrier Discharges. *Chem. Lett.* 30: 1304-1305.

Liu, C.J., Mallinson, R., Lobban, L. (1998). Nonoxidative Methane Conversion to Acetylene over Zeolite in A Low Temperature Plasma. *J. Catal.* 179:326-334.

Liu, C.J., Mallinson, R., Lobban, L. (1999a). Comparative Investigations on Plasma Catalytic Methane Conversion to Higher Hydrocarbons over Zeolites. *Appl. Catal. A: Gen.* 178: 17-27.

Liu, C.-J., Xu, G.-H. and Wang, T. (1999b). Non-Thermal Plasma Approaches in CO_2 Utilization. *Fuel Process. Technol.* 58: 119-134.

Liu, C.J., Marafee, A., Mallinson, R., and Lobban, L. (1997). Methane Conversion to Higher Hydrocarbons in A Corona Discharge over Metal Oxide Catalysts with OH Groups. *Appl. Catal. A: Gen.* 164:21-33.

Liu, C.J., Xue, B., Eliasson, B., He, F., Li, Y. and Xu, G.H. (2001b). Methane Conversion to Higher Hydrocarbons in the Presence of Carbon Dioxide using Dielectric Barrier-Discharge Plasmas. *Plasma Chem. Plasma Process.* 21: 301-309.

Liu, W., Xu, Y., Tian, Z. and Xu, Z. (2003). A Thermodynamic Analysis on the Catalytic Combustion of Methane. *J. Nat. Gas Chem.* 12: 237-242.

Liu, Y., Xue, J., Liu, X., Hou, R., and Li, S. (1998). In: Parmaliana, A. *et al*. (Eds.), Natural Gas Conversion V, *Studies in Surface Science and Catalysis 119*, Amsterdam: Elsevier Science B.V.

Lu, G., Shen, S. and Wang, R. (1996). Direct Oxidation of Methane to Methanol at Atmospheric Pressure in CMR and RSCMR. *Catal. Today*. 30**:** 41-48.

Lunsford, J.H. (2000). Catalytic Conversion of Methane to More Useful Chemicals and Fuels: A Challenge for the 21st Century. *Catal. Today*. 63: 165-174.

Lutz, A.E., Bradshaw, R.W., Bromberg, L. and Rabinovich, A. (2004). Thermodynamic Analysis of Hydrogen Production by Partial Oxidation Reforming. *Int. J. Hydrogen Energy*. 29: 809-816.

Lutz, A.E., Bradshaw, R.W., Keller, J.O. and Witmer, D.E. (2003). Thermodynamic Analysis of Hydrogen Production by Steam Reforming. *Int. J. Hydrogen Energy*. 28: 159-167.

Luyben, M.L. and Floudas, C.A. (1994). Analyzing The Interaction of Design and Control – 1. A Multiobjective Framework and Application to Binary Distillation Synthesis. *Comp. Chem. Eng.* 18: 933-969.

Lwin, Y., Daud, W.R.W., Mohamad, A.B., Yaakob, Z. (2000). Hydrogen Production from Steam-Methanol Reforming: Thermodynamic Analysis. *Int. J. Hydrogen Energy*. 25: 47-53.

Maiti, G.C. and Baerns, M. (1995). Dehydration of Sodium Hydroxide and Lithium Hydroxide Dispersed over Calcium Oxide Catalysts for the Oxidative Coupling of Methane. *Appl. Catal. A: Gen.* 127: 219-232.

Montgomery, D.C. (2001). *Design and Analysis of Experiments*. New York: John Wiley & Sons.

Muralidhar, R., Gummadi, S.N., Dasu, V.V. and Panda, T. (2003). Statistical Analysis on Some Critical Parameters Affecting the Formation of Protoplasts from the Mycelium of Penicillium Griseovulfum. *Biochem. Eng. J.* 16: 229-235.

Nandasana, A.D., Ray, A.K. and Gupta, S.K. (2003). Dynamic Model of an Industrial Steam Reformer and Its Use for Multiobjective Optimization. *Ind. Eng. Chem. Res.* 42: 4028-4042.

Nandi, S., Badhe, Y., Lonari, J., Sridevi, U., Rao, B.S., Tambe, S.S. and Kulkarni, B.D. (2004). Hybrid Process Modeling and Optimization Strategies Integrating

Neural Networks/Support Vector Regression and Genetic Algorithms: Study of Benzene Isopropylation on Hbeta Catalyst. *Chem. Eng. J.* 97: 115-129.

Nandi, S., Mukherjee, Tambe, S.S., Kumar, R. and Kulkarni, B.D. (2002). Reaction Modeling and Optimization Using Neural Networks and Genetic Algorithms: Case Study Involving TS-1 Catalyzed Hydroxylation of Benzene. *Ind. Eng. Chem. Res.* 41: 2159-2169.

Nozaki, T., Omata, K. and Fujimoto, K. (1990). Oxidative Coupling of Methane with Carbon Dioxide over Carbon Catalyst. *Fuel*. 69**:** 1459-1460.

Omran, Z.A. and Mohamed, M.M. (2002). Ceria-Modified Zirconia and Their Effects on the Molybdenum Oxide Dispersion. *Mat. Chem. Phys.* 77: 704-710.

Pareja, P., Molina, S., Amariglio, A. and Amariglio, H. (1998). Isothermal Conversion of Methane into Higher Hydrocarbons and Hydrogen by Two-step Reaction Sequence Involving A Rhodium Catalyst. *Appl. Catal. A: Gen.* 168: 289-305.

Pérez-Ramírez, J., Berger, R.J., Mul, G., Kapteijn, F. and Moulijn, J.A. (2000). The Six-Flow Reactor Technology: A Review on Fast Catalyst Screening and Kinetic Studies. *Catal. Today*. 60**:** 93-109.

Pietruszka, B. and Heintze, M. (2004). Methane Conversion at Low Temperature: The Combined Application of Catalysis and Non-Equilibrium Plasma. *Catal. Today*. 90:151-158.

Radhakrishnan, V.R. and Suppiah, S. (2004). Hammerstein Type Model of An Industrial Heat Exchanger. *Proceeding of the 18th Symposium of Malaysian Chemical Engineers*. December 13-14. Perak, Malaysia: Universiti Teknologi Petronas.

Raje, A., Inga, J.R. and Davis, B.H. (1997). Fischer-Tropsch Synthesis: Process Considerations Based on Performance of Iron-Based Catalysts. *Fuel*. 76: 273-280.

Ravi, V., Mok, Y.S., Rajanikanth, B.S., Kang, H.C. (2003). Temperature Effect on Hydrocarbon-Enhanced Nitric Oxide Conversion Using A Dielectric-Barrier Discharge Reactor. *Fuel Process. Technol.* 81:187-199.

Razavi, S.M.A., Mousavi, S.M. and Mortazavi, S.A. (2003). Dynamic Prediction of Milk Ultrafiltration Performance: A Neural Network Approach. *Chem. Eng. Sci.* 58: 4185-4195.

Reddy, B.M., Khan, A., Yamada, Y., Kobayashi, T., Loridant, S., and Volta, J.C. (2003). Structural Characterization of CeO_2-MO_2 ($M=Si^{4+}$, Ti^{4+}, and Zr^{4+}) Mixed Oxides by Raman Spectroscopy, X-ray Photoelectron Spectroscopy, and Other Techniques. *J. Phys. Chem. B*. 107: 11475-11484.

Richardson, J.T. (1989). *Principles of Catalyst Development*. New York: Plenum Press.

Ross, J.R.H., Keulen, A.N.J., Hegarty, M.E.S. and Seshan, K. (1996). The Catalytic Conversion of Natural Gas to Useful Products. *Catal. Today*. 30**:** 193-199.

Sarmidi, M.R., Aziz, R., Hussain, M.A., and Daud, W.R.W. (2001). Overview of Petrochemical Based Industries in Malaysia. *ASEAN J. Chem. Eng.* 204 (2): 143-152.

Schütze, A., Jeong, J.Y., Babayan, S.E., Park, J., Selwyn, G.S., and Hicks, R.F. (1998). The Atmospheric-Pressure Plasma Jet: A Review and Comparison to Other Plasma Sources. *IEEE Trans. Plasma Sci.* 26:1685-1694.

Silva, C.M. and Biscaia, Jr. E.C. (2003). Genetic Algorithm Development for Multi-Objective Optimization of Batch Free-Radical Polymerization Reactors. *Comp. Chem. Eng.* 27: 1329-1344.

Smith, J.M., Van Ness, H.C., and Abbott, M.M. (2001). *Introduction to Chemical Engineering Thermodynamics*. New York: McGraw Hill Book Co.

Song, C. (2001). Tri-Reforming: A New Process Concept for Conversion and Utilization of CO_2 in Flue Gas without Pre-Separation. *Chem. Innov.* 31**:** 212-226.

Song, H.K., Lee, H., Choi, J.W., and Na, B.K. (2004). Effect of Electrical Pulse Forms on the CO_2 Reforming of Methane using Atmospheric Dielectric Barrier Discharge. *Plasma Chem. Plasma Process.* 24: 57-72.

Stagg-William, S. M. (1999). *Novel Catalytic Materials for Carbon Dioxide Reforming of Methane under Severely Deactivating Conditions*. University of Oklahoma: PhD Dissertation.

Stephanopoulos, G. and Han, C. (1996). Intelligent System in Process Engineering: A Review. *Comp. Chem. Eng.* 20: 743-791.

Suhartanto, T., York, A.P.E., Hanif, A., Al-Megren, H. and Green, M.L.H., (2001). Potential Utilisation of Indonesia's Natuna Natural Gas Field via Methane Dry Reforming to Synthesis Gas. *Catal. Letters*. 71: 49-54.

Summanwar, V.S., Jayaraman, V.K., Kulkarni, B.D., Kusumakar, H.S., Gupta, K. and Rajesh, J. (2002). Solution of Constrained Optimization Problems by Multi-Objective Genetic Algorithm. *Comp. Chem. Eng.* 26: 1481-1492.

Sun, C., Li, H., Wang, Z., Chen, L. and Huang, X. (2004). Synthesis and Characterization of Polycrystalline CeO_2 Nanowires. *Chem. Lett.* 33: 662-663.

Tanabe, K., Misono, M., Ono, Y. and Hattori, H. (1989). New Solid Acids and Bases. in Delmon, B. and Yates, J.T. Eds. *Studies in Surface Science and Catalysis 51*. Tokyo: Elsevier Science Publishers. Kodansha, Ltd.

Tang, H. and Kitagawa, K. (2005). Supercritical Water Gasification of Biomass: Thermodynamic Analysis with Direct Gibbs Free Energy Minimization. *Chem. Eng. J.* 106: 261-267.

Tarafder, A., Rangaiah, G.P., and Ray, A.K. (2005). Multiobjective Optimization of An Industrial Styrene Monomer Manufacturing Process. *Chem. Eng. Sci.* 60: 347-363.

Tarca, L.A., Grandjean, B.P.A., and Larachi, F. (2002). Integrated Genetic Algorithm – Artificial Neural Network Strategy for Modelling Important Multiphase-Flow Characteristics. *Ind. Eng. Chem. Res.* 41: 2543-2551.

Terribile, D., Trovarelli, A., Leitenburg, C.D., Primavera, A. and Dolcetti, G. (1999). Catalytic Combustion of Hydrocarbons with Mn and Cu-Doped Ceria–Zirconia Solid Solutions. *Catal. Today*. 47: 133-140.

The MathWorks. (2001). *MATLAB Optimization Toolbox User's Guide*. Natick, MA.: The MathWorks, Inc.

The Mathworks. (2005). *Genetic Algorithm and Direct Search Toolbox for Use with MATLAB*. Natick, MA: The Mathworks, Inc.

Trovarelli, A., Leitenburg, C.D., Dolcetti, G., LLorca, J. (1995). CO_2 Methanation under Transient and Steady-State Conditions over Rh/CeO_2 and CeO_2-Promoted Rh/SiO_2: The Role of Surface and Bulk Ceria. *J. Catal.* 151: 111-124.

Valigi, M., Gazzoli, D., Pettiti, I., Mattei, G., Colonna, S., de Rossi, S. and Ferraris, G. (2002). WO_x/ZrO_2 Catalysts: I. Preparation, Bulk and Surface Characterization. *Appl. Catal. A: Gen.* 231: 159-172.

Vasudeva, K., Mitra, N., Umasankar, P. and Dhingra, S.C. (1996). Steam Reforming of Ethanol for Hydrogen Production: Thermodynamic Analysis. *Int. J. Hydrogen Energy.* 21: 13-18.

Wach, I.E. (1996). Raman and IR Studies of Surface Metal Oxide Species on Oxide Supports: Supported Metal Oxide Catalysts. *Catal. Today*., 27: 437-455.

Wang, J.G., Liu, C.J., Eliasson, B. (2004). Density Functional Theory Study of Synthesis of Oxygenates and Higher Hydrocarbons from Methane and Carbon Dioxide Using Cold Plasmas. *Energy Fuels*. 18:148-153.

Wang, S. and Zhu, Z.H. (2004). Catalytic Conversion of Alkanes to Olefins by Carbon Dioxide Oxidative Dehydrogenation – A Review. *Energy Fuels*. 18: 1126-1139.

Wang, Y. and Ohtsuka, Y. (2000). CaO-ZnO Catalyst for Selective Conversion of Methane to C_2 Hydrocarbons Using Carbon Dioxide as the Oxidant. *J. Catal.* 192: 252-255.

Wang, Y. and Ohtsuka, Y. (2001). Mn-based Binary Oxides as Catalyst for the Conversion of Methane to C_{2+} Hydrocarbon with Carbon Dioxide as an Oxidant. *Appl. Catal. A: Gen.* 219**:** 183-193.

Wang, Y., Takahashi, Y. and Ohtsuka, Y. (1998a). Carbon Dioxide-Induced Selective Conversion of Methane to C_2 Hydrocarbons on CeO_2 Modified with CaO. *Appl. Catal. A: Gen.* 172**:** L203-L206.

Wang, Y., Takahashi, Y. and Ohtsuka, Y. (1998b). Effective Catalyst for Conversion of Methane to Ethane and Ethylene Using Carbon Dioxide. *Chem. Lett.* 27: 1209-1210.

Wang, Y., Zhuang, Q., Takahashi, Y. and Ohtsuka, Y. (1998c). Remarkable Enhancing Effect of Carbon Dioxide on the Conversion of Methane to C_2 Hydrocarbons using Praseodymium Oxide. *Catal. Lett.* 56**:** 203-206.

Wang, Y., Takahashi, Y. and Ohtsuka, Y. (1999). Carbon Dioxide as Oxidant for the Conversion of Methane to Ethane and Ethylene Using Modified CeO_2 Catalyst. *J. Catal.* 186**:** 160-168.

Warsito, W. and Fan, L.S. (2003). Neural Network Multi-Criteria Optimization Image Reconstruction Technique (NN-MOIRT) for Linear and Non-Linear Process Tomography. *Chem. Eng. Process.* 42: 663-674.

Weissermel, K. and Arpe, H.J. (2003). *Industrial Organic Chemistry*. 4th Ed. Weinheim: Wiley-VCH GmbH & Co.

Wen, Y., and Jiang, X. (2001). Decomposition of CO_2 Using Pulsed Corona Discharges Combined with Catalyst. *Plasma Chem. Plasma Process.* 21:665-678.

Wilhelm, D.J., Simbeck, D.R., Karp, A.D. and Dickenson, R.L. (2001). Syngas Production for Gas-to-Liquids Applications: Technologies, Issues and Outlook. *Fuel Process. Technol.* 71**:** 139-148.

Wolf, E.E. (1992). *Methane Conversion by Oxidative Processing – Fundamental and Engineering Aspects*. New York: Van Nostrand Reinhold.

Wolfovich, M.A., Landau, M.V., Brenner, A. and Herskowitz, M. (2004). Catalytic Wet Oxidation of Phenol with Mn-Ce-Based Oxide Catalysts: Impact of Reactive Adsorption on TOC Removal. *Ind. Eng. Chem. Res.* 43: 5089-5097.

Wu, D., Li, Y., Shi, Y., Fang, Z., Wu, D. and Chang, L. (2002). Effects of the Calcination Conditions on the Mechanical Properties of a $PCoMo/Al_2O_3$ Hydrotreating Catalyst. *Chem. Eng. Sci.* 57: 3495-3504.

Xiong, Q. and Jutan, A. (2003). Continuous Optimization Using A Dynamic Simplex Method. *Chem. Eng. Sci.* 58: 3817-3828.

Yang, X. (1995). *A Spectroscopic Study of Methane Oxidative Coupling Catalysts*. Texas A&M University: PhD Dissertation.

Yao, H.M., Vuthaluru, H.B., Tadé, M.O. and Djukanovic, D. (2005). Artificial Neural Network-Based Prediction of Hydrogen Content of Coal in Power Station Boilers. *Fuel*. 84: 1535-1542.

Yao, S.L., Ouyang, F., Nakayama, A., Suzuki, E., Okumoto, M. and Mizuno, A. (2000). Oxidative Coupling and Reforming of Methane with Carbon Dioxide Using a High-Frequency Pulsed Plasma. *Energy Fuels*. 14: 910-914.

Yao, S.L., Suzuki, E., Meng, N., Nakayama, A. (2002). A High-Efficiency Reactor for the Pulsed Plasma Conversion of Methane. *Plasma Chem. Plasma Process.* 22: 225-237.

Youness, E.A. (2004). Characterization of Efficient Solutions of Multi-Objective E-Convex Programming Problems. *Appl. Math. Comp.* 151: 755-761.

Yu, W., Hidajat, K. and Ray, A.K. (2003). Application of Multiobjective Optimization in The Design and Operation of Reactive SMB and Its Experimental Verification. *Ind. Eng. Chem. Res.* 42: 6823-6831.

Zaman, J. (1999). Oxidative Processes in Natural Gas Conversion. *Fuel Process. Technol.* 58: 61-81.

Zeng, Y., Akin, F.T. and Lin, Y.S. (2001). Oxidative Coupling of Methane on Fluorite-Sructured Samarium-Yttrium-Bismuth Oxide. *Appl. Catal. A: Gen.* 213**:** 33-45.

Zhang, X., Dai, B., Zhu, A., Gong, W. and Liu, C. (2002a). The Simultaneous Activation of Methane and Carbon Dioxide to C_2 Hydrocarbons under Pulse Corona Plasma over La_2O_3/γ-Al_2O_3 Catalyst. *Catal. Today*. 72**:** 223-227.

Zhang, Z., Hidajat, K. and Ray, A.K. (2002b). Multiobjective Optimization of SMB and Varicol Process for Chiral Separation. *AIChE J.* 48: 2800-2816.

Zhang, K., Eliasson, B., and Kogelschatz, U. (2002c). Direct Conversion of Greenhouse Gases to Synthesis Gas and C_4 Hydrocarbons over Zeolite HY Promoted by a Dielectric-Barrier Discharge. *Ind. Eng. Chem. Res.* 41:1462-1468.

Zhang, K., Kogelschatz, U. and Eliasson, B. (2001). Conversion of Greenhouse Gases to Synthesis Gas and Higher Hydrocarbons. *Energy Fuels*. 15: 395-402

Zhao, W., Chen, D. and Hu, S. (2000). Optimizing Operating Conditions Based on ANN and Modified Gas. *Comp. Chem. Eng.* 24: 61-65.

Zhou, L.M., Xue, B., Kogelshatz, U., Eliasson, B. (1998). Non-Equilibrium Plasma Reforming of Greenhouse Gases to Synthesis Gas. *Energy Fuels*. 12:1191-1199.

Zhu, H., Qin, Z., Shan, W., Shen, W. and Wang, J. (2004). Pd/CeO_2–TiO_2 Catalyst for CO Oxidation at Low Temperature: a TPR Study with H_2 and CO as Reducing Agents. *J. Catal.* 225: 267-277.

Zou, J.-J., Zhang, Y., Liu, C.-J., Li, Y. and Eliasson, B. (2003). Starch-enhanced Synthesis of Oxygenates from Methane and Carbon Dioxide Using Dielectric-barrier Discharges. *Plasma Chem. Plasma Process.* 23: 69-82.